Final Progress Report

Project Title:	Energy Saving Separations Technologies for the Petroleum Industry: An Industry-University-National Laboratory Research Partnership
Covering Period:	11/1/00-10/31/02
Date of Report:	March 27, 2003
Contract ID Number:	DE-FC07-01ID13998
Subcontractors:	N/A
Other Partners:	Dr. Paul Bryan, ChevronTexaco, Richmond, CA; Dr. George Huff, BP Aromatics Group, Naperville, IL; Dr. Fred Stewart, INEEL, Idaho Falls, ID
Contact:	Profs. John R. Dorgan and J. Douglas Way Chemical Engineering and Petroleum Refining Dept. Colorado School of Mines 1500 Illinois Street Golden, CO 80401-1887 Phone: 303-273-3720, Fax: 303-273-3730
Project Team:	James Quinn, HQ Program Manager, james.quinn@hq.doe.gov

Project Objective: This project works to develop technologies capable of replacing traditional energy-intensive distillations so that a 20% improvement in energy efficiency can be realized. Consistent with the DOE sponsored report, Technology Roadmap for the Petroleum Industry, the approach undertaken is to develop and implement entirely new technology to replace existing energy intensive practices. The project directly addresses the top priority issue of developing membranes for hydrocarbon separations.

The project is organized to rapidly and effectively advance the state-of-the-art in membranes for hydrocarbon separations. The project team includes ChevronTexaco and BP, major industrial petroleum refiners, who will lead the effort by providing matching resources and real world management perspective. Academic expertise in separation sciences and polymer materials found in the Chemical Engineering and Petroleum Refining Department of the Colorado School of Mines is used to invent, develop, and test new membrane materials. Additional expertise and special facilities available at the Idaho National Engineering and Environmental Laboratory (INEEL) are also exploited in order to effectively meet the goals of the project. The proposed project is truly unique in terms of the strength of the team it brings to bear on the development and commercialization of the proposed technologies.

Background: Petroleum refining is the nation's most energy intensive industry. Estimates for 1994 indicate that the Petroleum industry used 6.3 quads (quadrillion BTU) [1]. Of this, atmospheric and vacuum distillation accounted for 35-40 percent of the total. Crude oils vary in content based on the place of origin and must be refined and separated into useful components. Currently this is primarily done by distillation, a process in which the fluids must be heated until boiling. This is the primary reason for the high energy costs associated with the refining process.

Membranes do offer an alternative means of separating chemical components without the need to heat and boil the fluids. Correspondingly, the energy savings associated with using a membrane separation process rather than distillation are enormous. Membrane separations rely on differences in the rate at which components pass through the membrane material. If one component passes through (or permeates) faster than another, the fast permeating species can be separated form the slower permeating species. There are several variations of this phenomena ranging from reverse osmosis, to ultrafiltration, or electrodiaysis. However, this proposal is concerned with improvements in *pervaporation* and in *gas separations*. Accordingly only these technologies in reference to refinery separations are reviewed here. The use of membrane separations in refinery operations has increased in recent years.

Pervaporation is a membrane process in which a liquid phase is in contact with one side of the membrane and the permeant side contacts a reduced pressure gas phase. Pervaporation has enjoyed great success in removing low amounts of water from organics, particularly in the dehydration of ethanol . Many commercial systems for this important application are available. In addition, these systems may be used to dehydrate a variety of organic materials including but not limited to methanol, butanol, xylenes, methylethylketone, tetrahydrofuran, and methylene chloride. Pervaporation is also used commercially to remove organics from aqueous streams. A colorful success story being the GFT process for the removal of ethanol from beer and wine in order to produce alcohol free beverages [2]. Technologies associated with organic/organic separations using pervaporation are much less developed with a significant shortfall being that known membrane materials have difficulty withstanding the needed operating conditions (prolonged high temperature exposure to organic solvents). Correspondingly, pervaporation has had less of an impact in refinery operations but holds tremendous potential for energy and associated costs savings if membranes can be constructed that are both effective and *robust*. It is because of this potential that the development of membranes for hydrocarbon separations ranks as one of the top two priorities in the *Technology Roadmap for the Petroleum Industry* document. A previous DOE sponsored research needs assessment specifically identified the development of pervaporation membranes for organic separations as the highest priority [3].

Presently, the biggest technical obstacle associated with pervaporation membranes is their inability to hold up under the conditions required for refinery relevant chemical separations. That is, known materials suffer from physical and chemical changes as a result of exposure to organic liquids and elevated temperatures. The proposed project addresses the relevant materials science issues for membrane materials so that effective and robust membranes capable of performing hydrocarbon separations can be manufactured and deployed.

In the context of refinery operations, gas separation membranes saw their first widespread commercial use in hydrogen recovery [4, 5]. Hydrogen is increasingly needed to process heavy and sour crudes making this an increasingly important area for innovation. Existing commercial systems (which are or have been available from several companies including Air Products, Union Carbide, and DuPont) are relatively easy to operate and require only modest capital investment. Several polymeric materials have been used in this context including aromatic polyamides, polyimides, and even cellulose acetate. Membrane separations have also been applied to the removal of carbon dioxide (CO_2) from various streams. For example, membranes

have been used to remove CO_2 from reformer offgas [6]. Several commercial systems are also available to separate CO_2 and methane (CH_4) an operation of immense importance in natural gas processing.

Status:

Rubbery Blend Membranes for Hydrocarbon Separations by Pervaporation: Utilization of membranes offers the promise of extraordinary energy savings if successfully applied to hydrocarbon-hydrocarbon and other organic separations. Membranes are bound to enter into refining and petrochemical operations involving liquid separations once appropriate materials and modules are developed. Hybrid processes such as utilizing membrane modules to break azeotropes formed during distillation are particularly attractive because they offer less process complexity and reduced capital investment [7, 8]. Such an approach is now accepted in the case of dehydration of ethanol as evidenced by the successful GFT process. Additionally, membranes are now available that can be used to reduce sulfur content in gasoline as evidenced by the introduction of the Sbrane™ process by the W.R. Grace company [9]. While presently limited in commercial application, these emerging success stories present an optimistic view for the future of membrane-based separations of organic liquids in demanding environments.

A common difficulty in utilizing membranes to separate organic liquids is that many common polymeric materials cannot withstand long-term exposure to organic liquids at the moderately high temperatures that are desirable. Excessive swelling of the polymers by organic liquids can produce selectivity losses. In extreme conditions, the membrane material may simply dissolve. If glassy polymers are used for separating liquids, a finite solubility of the organic will plasticize the polymer and lead to both selectivity and mechanical property losses. The need for robust membrane materials that are capable of withstanding exposure to the organic liquids has been identified as one of the primary obstacles in achieving organic separations utilizing membrane materials [3].

The approach taken in the present research and development project is to use physical blends of rubbery materials that are crosslinked. Blending allows for control of the solubility selectivity of the membrane while chemical crosslinking provides sufficient robustness to meet technical requirements. It must be appreciated that the use of rubbery polymers inherently implies that separation selectivity will be primarily based on differences in solubility as opposed to differences in diffusivity. This premise is based on the fact that for the rubbery systems under consideration, the swelling is very large so that molecular mobility is very high. The concept associated with the present novel membranes is that by blending together different components considerable control over the solubility selectivity may be achieved. Furthermore, semi-quantitative thermodynamic modelling may be used as a guide for formulating blends for specific separations. In this paper, these ideas are applied to the benzene-cyclohexane system.

Table I. Physical properties of benzene and cyclohexane

		Benzene	Cyclohexane
Freezing point(oC)		5.5	6.6
Boiling point(oC)		80.1	80.7
Density (g/cm3)		0.8737	0.7786
Refractive Index, n25D		1.498	1.426
Viscosity (cP)		0.65	0.98
Surface Tension (dyn/cm)		28.2	25.3
Molar volume (cm3/mol)		89.4	108.7
Collision diameter		0.526	0.606
Solubility Parameters (MPa)1/2	δ_t	18.5	16.8
	δ_D	18.4	16.8
	δ_p	0.0	0.0
	δ_h	2.0	0.2

Benzene-cyclohexane separation is of interest for many reasons. Cyclohexane is physically very similar to benzene as demonstrated by the property comparison shown in Table I. As a result of the very close boiling points (0.6 C) and similar physical properties benzene and cyclohexane form an azeotrope and thus provide a good model for azeotrope breaking by pervaporation. In addition, the pair may be used to represent the separation of aromatics (benzene) from aliphatics (cyclohexane); a class of separations of technological importance.

Materials: Conceptually, many choices are available for rubbery blends. In this work, the membrane system chosen consisted of the ternary blend of styrene butadiene rubber (SBR) copolymer, acrylonitrile butadiene rubber (NBR) copolymer, and polyvinylchloride (PVC). This blend is known to have a wide range of miscibility; NBR and PVC are miscible in all proportions. Additionally, this blend system possesses excellent solvent and good heat resiliance.[10] NBRs and SBR were provided by Nippon Zeon and have 41.5, 28, 18% acrylonitrile content and 23.5% styrene content, respectively. PVC homopolymer was purchased from Aldrich Chemical Company.

NBR, SBR and PVC were dissolved in cyclohexanone to prepare a polymer blend solution of known composition. Prepared blend samples are designated numerically as parts NBR, SBR, PVC. For example, 712 represents the blend containing 70 wt% NBR, 10 wt% SBR and 20 wt% PVC. Crosslinking agents and when necessary, activator and accelerator, were added into the solution. The solution was cast onto glass plate and dried in a fume hood for apporximately 1 day (16-24 hours). This cast membrane film was crosslinked under vacuum in an oven at 130 °C for 80 minutes.

Methods: Screening of blend formulations was accomplished by simple swelling tests. Prepared membrane samples were massed and subsequently submerged into solvent in sealed Erlenmeyer flasks with agitation provided by a shaker table for 1 day at 25 °C. Upon removal,

the samples were blotted dry using a Kimwipe paper towel and immediately massed. The swelling ratio (SR) of was calculated with following equation,

$$Swelling\ Ratio\ =\ \frac{W_d - W_s}{W_d} \times 100 \tag{1}$$

where W_d and W_s are the weight of dry and swollen samples, respectively.

Pervaporation experiments were carried out with laboratory scale equipment consisting of a Millipore membrane holder having an effective membrane area in contact with the feed liquid of 13,8 cm^2. The feed liquid was continuously circulated from and returned to a 3 L reservoir. Downstream pressure was maintained below 5 torr, typically at about 2 torr. After an equilibration period of at least 6 hours, permeate was collected at constant time intervals by means of freezing in a liquid nitrogen cooled cold finger. Analysis of feed and permeation stream compositions was performed by Gas Chromatography – Mass Spectrometry (Agilent GC-MASS G2570A) and checked by simple refractive index measurements.

The separation factor(a) and permeation rate are defined in the usual manner as follows in Equations 1 and 2.

$$\alpha = \frac{w_{P,Benzene} \Big/ w_{P,cyclohexane}}{w_{F,Benzene} \Big/ w_{F,cyclohexane}} \tag{2}$$

$$Permeation\ Rate = Q = \frac{q \times L}{A \times t} \tag{3}$$

Here $w_{P,i}$ is the weight fraction of component i in permeate and $w_{F,i}$ is that in the feed. Q is the normalized flux or permeation rate where q, L, A and t represent the mass of collected permeate (g), membrane thickness (mm), membrane area (m^2) and operating time (in hours), respectively.

Theory: The theoretical approach taken rests on the transport mechanism of pervaporation following the solution-diffusion mechanism [11]. The relevant quantitative relationship is given by Equation (4).

$$J_i = \frac{D_i}{L}(c_{i0,m} - c_{iL,m}) = \frac{D_i K_i^{gas}}{L}(p_{i0} - p_{iL}) = \frac{P_i}{L}(p_{i0} - p_{iL}) \tag{4}$$

In Equation (4), J_i represents the flux of species *i*, *D* is diffusivity, *L* is the thickness of the membrane, and $c_{i0,m}$ represents the concentration of the species internal to the membrane at position 0 whereas $c_{iL,m}$ represents the concentration internal to the membrane at position L. The K_i^{gas} is a gas phase sorption coefficient that allows reference to the concentrations external to the membrane via the partial pressures on either side of the membrane, p_{i0} and p_{iL}. Finally in Equation (4), the gas permeability coefficient, P_i, is defined as the product of D_i and K_i^{gas}.

For complete thermodynamic generality, it should be remembered that the concentration internal to the membrane is related to the concentration external to the membrane by the quality of chemical potentials (μ),

$$\mu_{i,m} = \mu_i \quad (5)$$

Equation (5) is the rigorous basis for the form presented in Equation (4). Equation (4) reveals the basic physics exploited by the present approach. Namely, blending is performed in order to maximize the difference in the product of D_iK_i or in the case of solubility selectivity being dominant, directly in the values for $c_{i0,m}$. A fuller discussion of the quantitative methodology used to accomplish this goal is described below.

Results: Swelling kinetics are of interest for many reasons; a simple experiment is used to both determine the time needed to equilibrate the rubber and to determine diffusion coefficients for the pure solvents. Kinetics of mass uptake for benzene, cyclohexane, and a 50:50 weight mixture of the two are presented in Figure 1 for a 712 blend. Equilibrium swelling is achieved within 4 hours. Diffusion coefficients for benzene and cyclohexane in the blend are 1.12 X 10^{-12} m^2/sec and 1.92 X 10^{-13} m^2/sec, respectively. Published diffusion coefficient data for benzene in natural rubber is 1 X 10^{-11} m^2/sec while the value for benzene in PVC is 3 X 10^{-17} m^2/sec [12]. Accordingly, the values determined are within reasonable bounds.

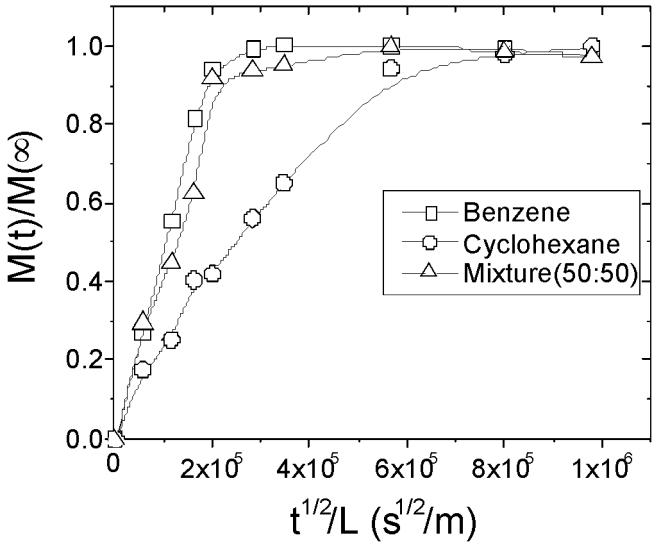

Figure 1. Mass update of components in blend 712.

Knowing that the blends are equilibrated, a systematic investigation of the relationship between swelling and blend composition can be undertaken. Figure 2 shows the results of swelling tests performed as the NBR content and, separately, the PVC content were changed in two series of blends. When the content of NBR is increased, the swelling of both benzene and cyclohexane are decreased. However, the ratio of benzene swelling to swelling by cyclohexane (the swelling selectivity) increases. The same is true for blends in which the PVC content is increased. These results are easily rationalized by realizing that NBR and PVC are polar in nature and thus preferentially solubilize benzene to cyclohexane.

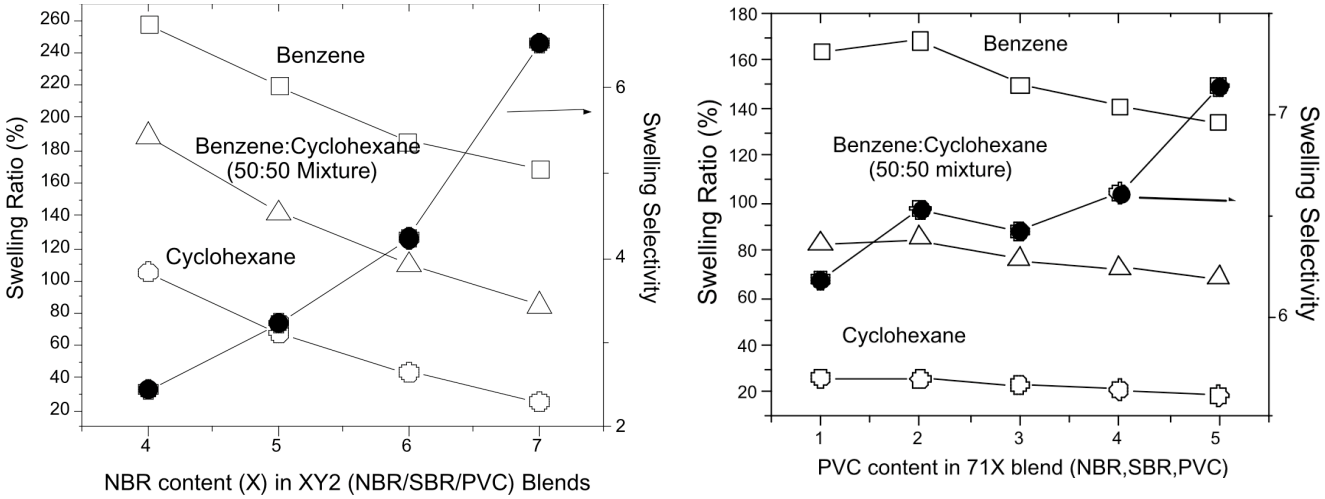

Figure 2. Effects of blend composition on equilibrium swelling.

The results of Figure 2 may be empirically described by utilizing the concept of the solubility parameter. This physical quantity is described for a low molecular weight compound according to Equation 6.

$$\delta = \left(\frac{E_{coh}}{V}\right)^{1/2} = \left(\frac{\Delta H_{VAP} - RT}{V}\right)^{1/2} \tag{6}$$

Here, δ is the solubility parameter, E_{coh} is the cohesive energy, V is volume, ΔH_{VAP} is the enthalpy of evaporation, R is the gas constant, and T is temperature. For polymers, the solubility parameter can be defined as equal to the value of the solvent that produces the maximum degree of swelling in a crosslinked version.

Solubility parameter values for the polymers used in this study are readily available and are often split into dispersion (δ_d), polar (δ_p) and hydrogen bonding (δ_h) components [13]. In the present study, it is convenient to define a parameter, δ_a, according to Equation 7.

$$\delta_a^2 = \delta_p^2 + \delta_h^2 \tag{7}$$

In addition, a simple blending rule for solubility parameters of the blends in the form of Equation 8 is also utilized,

$$\delta_{a,Blend} = \sum_i \varphi_i \delta_{a,i} \tag{8}$$

where φ_i represents the volume fraction of species *i*. Figure 3 presents the measured swelling selectivities as a function of the calculated polar component solubility parameter for several different blends. From this figure, it can be seen that a reasonably quantitative relationship between solubility selectivity and the polarity of the polymer blend does exist. This establishes a design heuristic for the separation of benzene and cyclohexane, namely, the blend should be made as polar as possible.

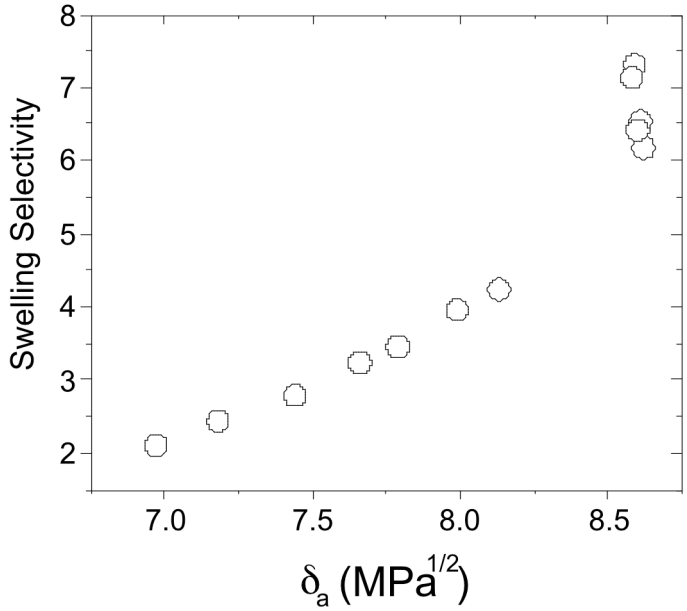

Figure 3. Selectivity versus polar components of the solubility parameter.

Careful inspection of Figure 3 reveals that the solubility parameter approach is limited in utility. Several blends have δ_a values around 8.6 $MPa^{1/2}$ but significantly different swelling selectivities. Accordingly, while solubility parameters are an easy way to screen blend materials they do not provide a rigorous, quantitative predictive capability.

Pervaporation results for a 50:50 by weight mixture of benzene and cyclohexane are exhibited in Figure 4. In this figure, the selectivity factor, α, defined by Equation 2 is plotted against the permeation rate defined by Equation 3. A typical tradeoff curve is found with fluxes increasing as selectivity decreases. It should be remembered that in this plot each point represents a different blend composition having a distinct performance. Attention should also be focused on the high permeation rates. In principle, a 10 μm permselective layer could produce between 0,5 and 5,0 kg/m^2hr at 25 C.

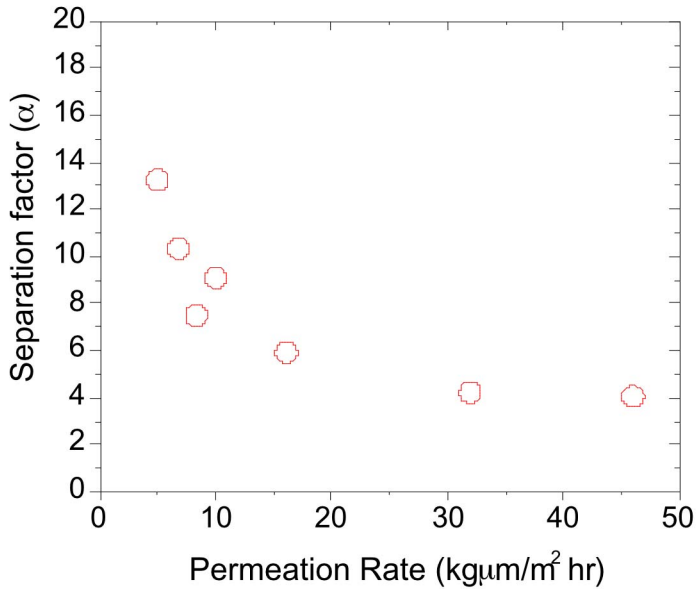

Figure 4. Pervaporation selectivities for a series of rubbery blend membranes.

The material with the highest selectivity in Figure 4 is blend 316. Therefore this blended material was investigated across different compositions of the benzene cyclohexane feed mixture; results are presented in Figure 5. Figure 5 also presents one data set for the 316 blend separating a 50:50 mixture at a temperature of 60 C. Increasing the temperature from 25 to 60 C results in a relatively small decrease in permeate concentration (from 93.9 to 88.3 wt.%) but to an enormous increase in permeation rate of nearly a factor of twenty (from 5.0 to 98.9 kg μm / m^2 hr). From a practical perspective this means that the azeotropic composition in the benzene-cyclohexane system can be enriched to greater than 85 wt.% at a productivity of nearly 10 (kg/m^2 hr) utilizing a 10 μm permselective layer of the optimised blend. To the authors' knowledge, this is the highest fluxing material able to achieve this level of separation reported to date.

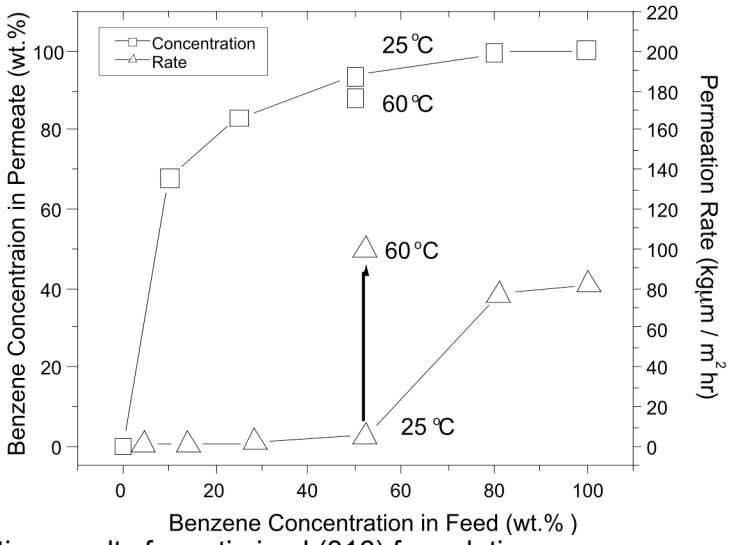

Figure 5. Pervaporation results for optimised (316) formulation.

A *predictive* approach to the formulation of blended membranes may be pursued through the utilization of group contribution methods. In particular, the UNIFAQ-FV model of Oishi and Prausnitz has been adopted to describe solubility of benzene and cyclohexane in the present blends [14]. This procedure is only briefly described here but a more exhaustive description is forthcoming [15].

The UNIFAQ model was initially established for liquid-vapor equilibrium calculations and then extended to predict phase behavior for polymer mixtures and solutions. In this model, the activity of a solution consists of three contributions.

$$\ln a^{Total} = \ln a^{C} + \ln a^{R} + \ln a^{FV} \tag{9}$$

Here, a^{Total} is the activity of a component, a^{C} represents the combinatorial contribution, a^{R} is a residual contribution and a^{FV} is the free-volume contribution to the total activity. The combinatorial contribution is an entropic mixing factor based on differences in the size and shape of dissimilar molecules.

$$\ln a_j^{C} = \ln \varphi + 1 - \sum_{j=1}^{q} \varphi_j \tag{10}$$

where φ_j represents the volume fraction of species *j*. The residual factor represents the enthalpy exchange between two groups.

$$\ln a_j^{R} = \sum_{k} \nu_k^{j} \left[\ln \Gamma_k - \ln \Gamma_k^{j} \right] \tag{11}$$

where ν^{j}_{k} is the number of groups of type *k* in molecule *j*, Γ_k is the group residual activity, and Γ^{j}_{k} is the group residual activity in a reference solution containing only molecules of type *j*. Finally, the free volume factor is given by Equation 12.

$$\ln a^{FV} = 3c_1 \ln\left[\frac{\tilde{v}_1^{\frac{1}{3}} - 1}{\tilde{v}^{\frac{1}{3}} - 1}\right] - c_1\left\{\left[\frac{\tilde{v}_1}{\tilde{v}} - 1\right]\left[1 - \frac{1}{\tilde{v}_1^{\frac{1}{3}}}\right]^{-1}\right\} \quad (12)$$

where $\tilde{v}$ is reduced volume fraction, $3c_1$ is the number of external degree of freedom per solvent molecule (for hydrocarbons this value is 1,1). The grand advantage of a group contribution methodology is that *predictions* about the relative solubilities of various compounds in a polymer blend can be made without the need for any data. Utilizing this approach allows for the formulation an optimal blend composition for arbitrary mixtures based on a solubility selectivity approach. The benefit of the group contribution methodology is apparent when examining the present pervaporation data.

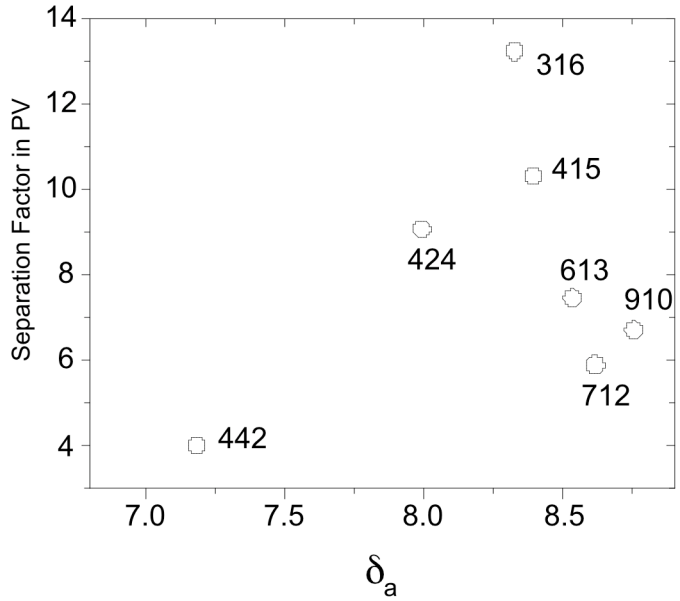

Figure 6. Pervaporation selectivity versus polar solubility parameter.

Figure 6 presents the pervaporation selectivity results plotted versus the polar components of the solubility parameter for the blends. In this figure individual blends are labeled. It is easily seen that the description of performance utilizing solubility parameters is inadequate. A non-monotonic relationship is found.

A much more satisfactory description is possible utilizing the UNIFAQ-FV model as evidenced in Figure 7. In this case, the equilibrium solubilities of benzene and cyclohexane were calculated using the UNIFAQ-FV model. That is, the rigorous phase equilibrium problem specified in Equation 5 has been solved for $c_{i,o}$ for both benzene and cyclohexane. This is an iterative calculation as the equilibrium concentration of benzene is affected by the concentration of cyclohexane and vice versa. From the equilibrium concentrations, solubility selectivity may be calculated. The correlation between measured membrane performance and calculated selectivity is very good.

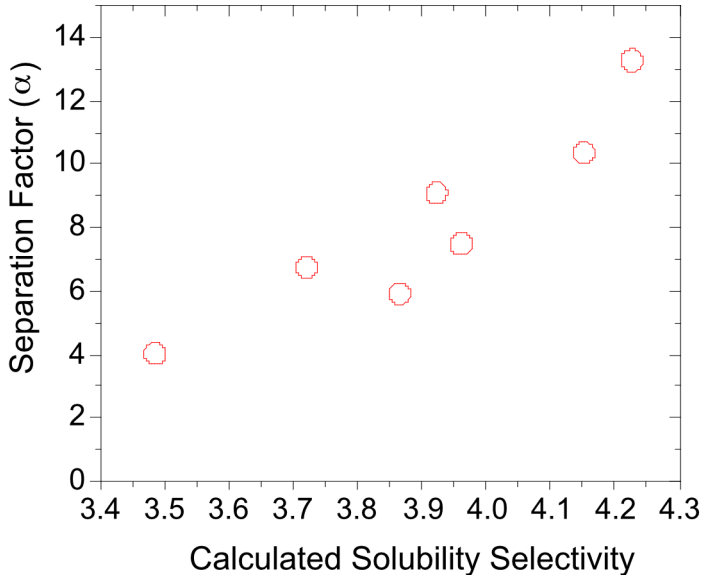

Figure 7. Pervaporation selectivity versus *a priori* calculated solubility selectivity.

A few comments on the significance of Figure 7 are warranted. First, it should be considered a great success in the sense that the calculation does provide a rigorous means of screening blend formulations in an *a priori* fashion. There exists a well-posed optimization problem for any separation of organic liquids in which it is desired to maximize solubility differences. Utilizing a group contribution method, solubility selectivities may be calculated as the blend formulation is changed. Figure 7 demonstrates that such a calculation does in fact reveal the optimal formulation of the blend. At a minimum, the approach can distinguish, in an *a priori* fashion, promising blend formulations in a quantitative way and thus reduce the number of needed experiments during membrane development.

The lack of better quantitative agreement in Figure 7 is also of interest. A shortcoming of the group contribution method used here is that no distinction is made between a CH_2 group in a cyclic (cyclohexane) versus linear (hexane or other aliphatic linear chain) structure. Previous reports have found that the UNIFAQ model overestimates the solubility of cyclohexane and this has led some researchers to change the parameter values for the CH_2 group in cyclic structures. In this work, the temptation to adjust parameters to better fit the data has been resisted in favor of a less quantitative but more predictive model. It should also be remembered that differences in diffusivity between benzene and cyclohexane may play a role in the actual pervaporation performance. The results of Figure 1 show that the pure component diffusivities differ by a factor of 5 in blend 712. On the downstream side of the membrane where penetrant concentrations are low, diffusion selectivity may become dominant. However, Figure 1 also shows that the 50:50 mixture of benzene and cyclohexane diffuses into the membrane at a rate nearly equal to that of benzene. It is anticipated that the present system is a case of coupled diffusion in which the rapidly diffusing species benzene swells the membrane material and facilitates the diffusion of cyclohexane. The role of diffusion selectivity in these blended

materials is under investigation. To date, a predictive approach to coupled diffusion in highly swollen rubber membranes remains elusive.

Conclusions: Membranes are entering into the demanding field of hydrocarbon separations as evidenced by the recent commercialization of pervaporation systems. The wide scale deployment of such systems holds the promise of tremendous energy savings and considerable associated environmental benefits. A limitation associated with greater usage is the lack of sufficiently robust membranes with acceptable mechanical and chemical properties. Additionally, the design of membrane materials from an *a priori* perspective for arbitrary separations remains an elusive goal of the membrane technical community.

In this project, a novel approach was undertaken that consisted of using blends of rubber polymers that are crosslinked in order to obtain sufficient mechanical and chemical robustness. The utilization of blended materials allows for a wide range of chemical functionality within the blend that can be exploited in order to produce the best possible solubility selectivity. Adoption of a group contribution thermodynamic model provides an *a priori* methodology for seeking the best blend formulation. While quantitative agreement with experiment is not achieved, the modeling does predict the best blend formulation and as such serves the needed role of providing a rational methodology for *designing* blend membranes for specific purposes.

The ideas put forth in this ongoing work have been demonstrated on the model system of benzene and cyclohexane. This system is of industrial interest in itself and also serves as a good model for both azeotrope breaking and aliphatic-aromatic separations. The optimized blend is capable of enriching a 50 wt.% mixture to 88.3 wt.% at a permeation rate of nearly 10 (kg / m^2 hr) utilizing a 10 μm permselective layer when operated at 60 C. This performance is among the best ever reported for the benzene-cyclohexane system.

Gas Separations Using Polyphosphazene Membranes: Removal of CO_2 and H_2S from CH_4 containing gas streams are primary goals of this research. The separation materials consist of asymmetric thin dense polymer film-ceramic composite membranes that have been studied for pure gas permeability and mixed gas separation performance. Ceramic substrates used in these studies are a commercially available controlled pore size alumina disk. Thin dense films are formed from a bulk polyphosphazene material that was applied using solution-casting techniques to form defect-free films. Typical film thicknesses range from 5 μm to 200 μm.

Polyphosphazenes are a unique class of hybrid organic-inorganic material that enjoys a high level of thermal and chemical stability required for use in the petrochemical industry. This inherent stability is due to the hybrid nature of the polymer where the inorganic backbone consists of alternating phosphorus and nitrogen atoms, see Figure 8. Bonding in the backbone consists of alternating double and single bonds and each phosphorus is pentavalent leaving two possible attachment points for pendant groups. Pendant groups provide the most evident chemical and physical properties. By varying the pendant groups, the chemical and physical properties are also varied.

The backbone is formed through the ring opening polymerization of commercially available hexachlorocyclotriphosphazene (1) yielding poly[(dichloro)phosphazene] (2). At each

phosphorus, there are two chlorines that displace readily through exposure to a nucleophile, such as water. Thus, the chloro polymer is hydrolytically unstable. Substitution of the chlorines for organic oxygen or nitrogen containing pendant groups yields durable stable materials (3) suitable for many applications. The transport properties have been known to be different with respect to pendant group. The goal of this work is to develop new materials for the removal of CO_2 and H_2S from CH_4 gas streams, and to fundamentally understand the mechanism of transport such that new systems can be envisioned, designed, and synthesized.

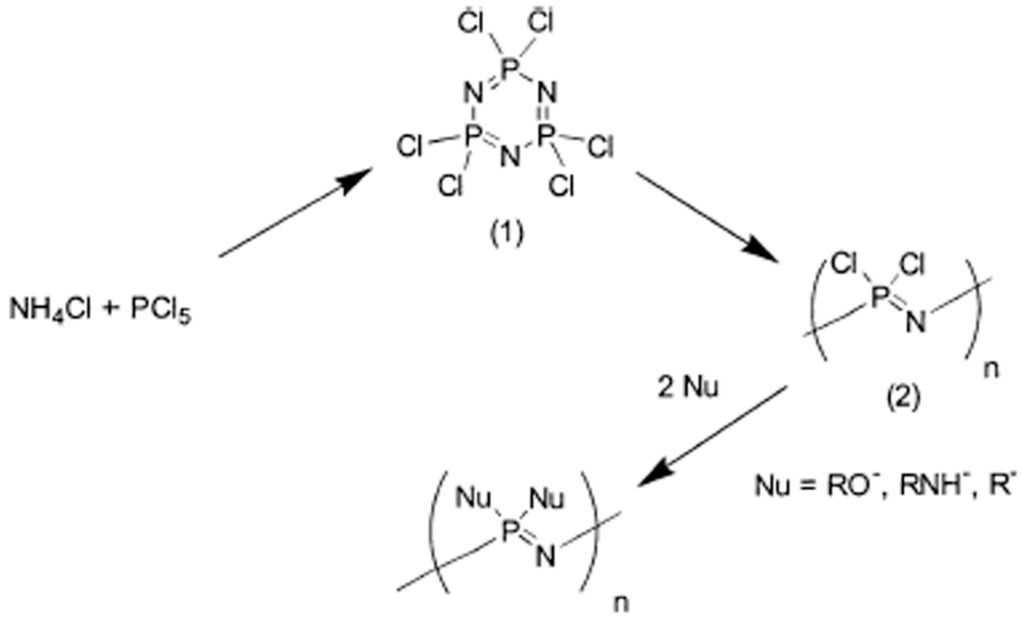

Figure 8. Synthesis of Polyphosphazenes.

Gas Permeability Experiments for MEE Substituted Phosphazenes. *Pure Gas Experiments*. Pure gas permeability determinations were conducted using the time-lag method [16, 17]. Measurements were made on thin dense films (200 μm thickness) installed into an apparatus as shown in Figure 9. The instrument is housed in a constant temperature enclosure and the temperature for all experiments was 30 C.

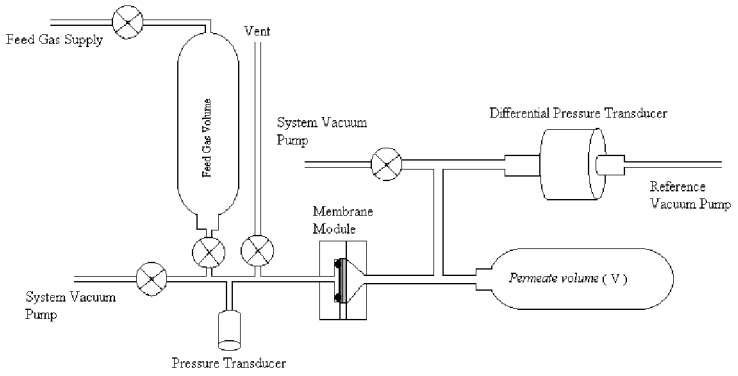

Figure 9. Schematic diagram of the pure gas permeability measurement instrument.

A series of related MEE substituted phosphazene polymers were studied for permeability and selectivity using both pure and mixed gas systems. Characterization of the polymer was accomplished through integration of their proton Nuclear Magnetic Resonance (NMR) spectra (Table 1). These polymers have three differing pendant groups attached each with a specific function. 2-(2-methoxyethoxy)ethanol (MEE) is a polar aprotic organic pendant group that has been correlated to CO_2 permeability in previous work [18]. 4-Methoxyphenol is hydrophobic and assures good film forming performance. 2-Allylphenol provides functionality for facile cross-linking. In general, the polymer series consists of an increasing polar MEE percentage while decreasing the non-polar 4-methoxyphenol, thus increasing the polarity of the polymer.

Table 1. Composition of Substituted Polyphosphazenes.

Polymer	MEE (%)	4-Methoxyphenol (%)	2-Allylphenol (%)
M2A	6	75	19
M010	21	72	7
M2B	38	46	16
M2D	48	48	4
M2E	74	24	2

Pure gas permeabilities were measured for these polymers where increasing permeability for CO_2 was noted with increasing MEE in the polymer. In fact, increases in permeability for all gases tested was observed with increasing MEE, although the other gases have an overall lower permeability than CO_2 (Table 2). Additionally, CO_2/Ar and CO_2/CH_4 ideal gas selectivities remained approximately constant.

Table 2. Pure Gas Permeabilities (in Barrers) and Ideal Selectivities.

Polymer	O_2	Ar	CH_4	CO_2	α CO_2/Ar	α CO_2/CH_4
M2A	1.6	1.3	1.2	13.5	10.4	11.3
M010	12.3	9.2	4.5	47.6	5.2	10.6
M2D	18.1	16.0	24.8	241.5	15.1	9.7
M2E	17.3	17.5	24.3	237.9	13.6	9.8

Mixed Gas Experiments. Mixed gas tests have been carried out to directly measure selectivity. As illustrated in Figure 10, a feed gas is flowed across one side of a membrane at a rate of 4 ml/min. Adjustment between the feed gas regulator and the mass flow controller determine the pressure and feed flow on the membrane. The feed gas pressure for these experiments was 30 psi. Gases that permeate through the membrane are swept away in a helium gas stream. The permeate sweep gas flow is also controlled by a mass flow controller, and is set at 2 ml/ min. The total permeate flow during testing is measured directly using an electronic soap bubble meter. Both the permeate and feed flows are directed by a series of automated valves through two different gas chromatographs (GC) equipped with different detectors for analysis. GC A is equipped with flame ionization detectors (FID) for the analysis volatile organics, while GC B has thermal conductivity detectors (TCD) for analyzing permanent gases. The test valves and membrane were housed in an oven to maintain a constant temperature of 30 C.

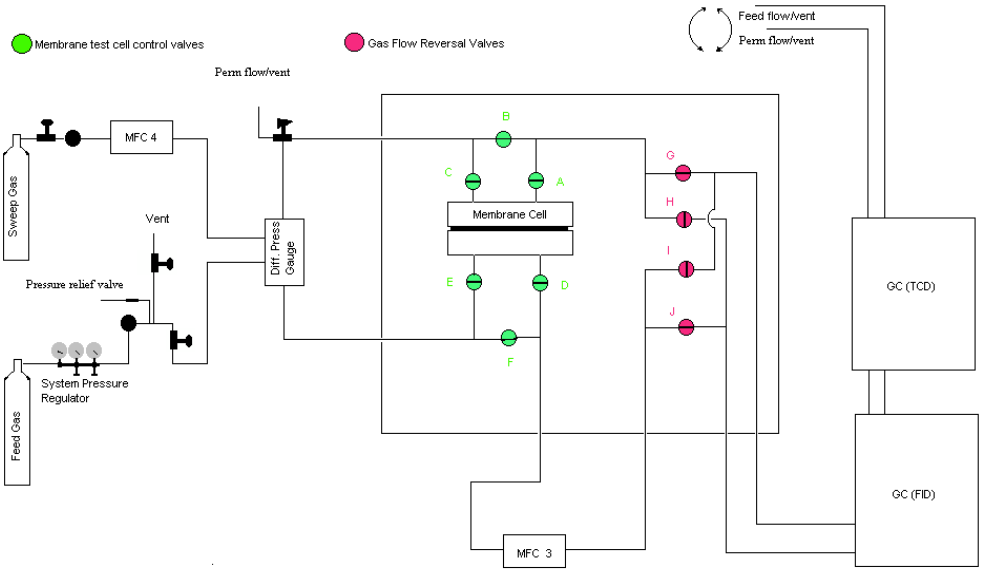

Figure 10. Schematic diagram of the mixed gas membrane test apparatus.

Note: The flow for channel A was plumbed to allow the exit flow from the injection valve to go into the entry port for the injection valve for channel B. This allows both the perm and feed to go through each column in GC B at the same time.

Permeabilities were calculated using eq. 1, where: $\Delta V/\Delta t$ is the total flow per unit time through the membrane, $T_{exp}\, P_{stp} / T_{stp}\, P_{exp}$ corrects to standard temperature and pressure, *l* is membrane thickness, A is membrane area, and Δp_1 is the pressure differential taken from the feed pressure and concentration determined from the GC analysis. In this study, a gas mixture consisting of 3% of each of the following gases: argon, oxygen, nitrogen, methane, and carbon dioxide, with the balance consisting of helium, was used for all measurements.

$$p = \frac{\Delta V}{\Delta t}\frac{T_{\exp} P_{stp}}{P_{\exp} T_{stp}}\frac{l}{A\Delta p_1} \qquad (13)$$

Trends between structure and gas permeability are not as clear as seen for the pure gas experiments (Table 3). This was not unexpected due the intermolecular interactions between the gases. However, the CO_2/Ar selectivities remained roughly consistent with the ideal selectivities. Nitrogen data was omitted from this study due to poor correlation to the rest of the data set. It is proposed that nitrogen contamination from the atmosphere skewed the data. Permeabilities of oxygen may also be somewhat questionable, especially the data for polymer M2E. A permeability of 120 Barrers compares poorly with the corresponding pure gas data point.

Table 3. Mixed Gas Permeabilities (in Barrers) and Selectivities.

Polymer	O_2	Ar	CH_4	CO_2	α CO_2/Ar	α CO_2/CH_4
M2A	26.8	2.8	4.8	8.4	3.0	1.8
M010	9.6	1.2	3.6	10.8	9.0	3.0
M2B	7.8	1.9	3.9	24.5	12.9	6.3
M2D	12.4	3.8	7.3	54.0	14.2	7.4
M2E	120	18.1	57.2	214	11.8	3.7

Gas Permeability of Fluorinated Phosphazenes. Poly[trifluoroethoxyphosphazene] (PTFEP) and a mixed fluorophosphazene elastomer, Eypel-F™ were characterized under pure and mixed gas conditions (Table 4). These fluorinated polymers are characterized by higher gas permeabilities when compared to all but the highest MEE content polymer (M2E). Permeabilities between the two measurement modes correspond well and the separation factors are consistent. In the mixed gas experiments, the oxygen permeabilities appear high, however this is consistent with the previous data and with contamination as a possible cause. Good permeabilities were measured for CO_2 suggesting a solubility interaction with both polymers.

Table 4. Pure and Mixed Gas Data for PTFEP and Eypel-F.

Polymer	Method	O_2	Ar	CH_4	CO_2	α CO_2/Ar	α CO_2/CH_4
PTFEP	Pure	81.3	67.6	46.9	420	6.2	9.0
PTFEP	Mixed	120	58	54	351	6.1	6.5
Eypel-F™	Pure	65.1	37.2	40.6	376	10.1	9.3
Eypel-F™	Mixed	153	65	78	403	6.2	5.2

Chemically Modified Ceramic Membranes for Xylene Separations: Effective separation of positional isomers has been an important problem in the petroleum industry. The xylene isomers are separated in industry using distillation methods, adsorption processes or crystallization methods. However, since they are complex and energy consuming, membrane separation techniques have been widely investigated as possible replacements. Zeolite membranes[19-21], polymeric membranes[22-28] and liquid membranes[29, 30] have been reported for the separation of hydrocarbon mixtures or mixtures of aromatic hydrocarbons.

A promising new class of complexation agents for the separation of positional isomers are cyclodextrins (CD) that have the structure of doughnut-shaped rings consisting of 6-8 glucose units. The CD cavity can accommodate various aromatic carbon molecules [31]. Because of their higher selectivity, CD modified materials have been commercialized as column packing materials for high performance liquid chromatography (HPLC) and capillary gas chromatography[32, 33]. However, their use in the industrial scale process for the separation of isomers has not been accomplished because of the difficulty of handling inclusion complexes[34, 35]. Therefore, we have investigated a continuous separation process using CD modified membranes.

Krieg et al.[27] described a porous, ceramic, tubular membrane impregnated with a β-CD polymer for the separation of the racemic pharmaceutical chlorthalidone. They impregnated β-CD into the pores of Al_2O_3 and Zr_2O_3 composite membranes and polymerized the impregnated CDs using epichlorohydrin. They obtained an average separation factor of 1.24 and the selectivity was consistent with the elution order observed in chiral HPLC. They speculated that the separation occurred based on selective inclusion of penetrants within the CD cavity, where the strongly interacting component might be captured, which would make its diffusivity in the membrane slower than that of the less interacting component. They also mentioned that the less interacting component might diffuse through the center of the channel without inclusion into the CD. Their suggested separation mechanism means that the selectivity was determined based on the difference of diffusivity between the permeating components.

Polymer and β-CD composite membranes have been reported. Miyata et al. [26] reported poly(vinyl alcohol) (PVA) membranes containing β-CD for the separation of *o*-/*p*-xylene binary mixtures. Evapomeation tests using this membrane showed that a mixture of 10 wt% *p*-xylene was concentrated to about 30 wt%. The selectivity of *p*-xylene increased as the *p*-xylene concentration in feed decreased from 100 wt% to 10 wt%. They concluded that the selectivity of p-xylene permeation was high at low concentration because the contribution of the flux through the PVA matrix becomes small as the p-xylene concentration decreased in the feed.

Yamasaki et al.[24] also reported similar membranes for the separation of ethanol/water mixtures using pervaporation. They observed a significant dependence of the flux on the ethanol concentration in feed. It was concluded that this dependency was due to the change of diffusivity of both components based on theoretical analyses with a solution-diffusion model using the sorption data.

Chen et al.[25] has reported the separation of xylene isomers using β-CD filled PVA membranes. They investigated the selectivity and flux for feed streams containing 5 % - 35 % p-xylene concentration during pervaporation of *p*-/*m*-xylene binary mixtures. The selectivity showed a maximum at 10 wt% feed p-xylene and the flux increased as the concentration of p-xylene in the feed increased. From the similarity of the change of flux with the solubility change of *p*-xylene, they concluded that pervaporation was mainly influenced by the formation of xylene inclusion complexes in the CD cavity.

Although a comparison of the reported results on inorganic and polymeric CD modified membranes is not straightforward because the influence of swelling in polymeric membranes would significantly influence their performance, the detailed separation mechanism of CD modified membranes is still obscure and a mathematical model has not been developed yet. In this paper, we describe β-CD modified ceramic membranes for the separation of xylene mixtures including pervaporation data using this membrane and a mathematical model to predict its performance using transport theory and molecular simulation techniques. A mathematical model was formulized based on Stefan-Maxwell theory assuming a surface-diffusion model. Model parameters including sorption isotherms were obtained from experiments, and the intrinsic thermal diffusion coefficients based on Stefan-Maxwell theory were obtained from molecular dynamics simulations. We will describe how this model can reproduce the experimental observations including the selectivity and fluxes.

Theory: The selectivity of a CD modified membrane is hypothesized to depend on the inclusion dynamics in the CD cavity whose size is close to the xylene molecule. The molecules permeating through the membrane would be captured in a CD cavity first, and then would move to a neighboring CD cavity according the driving force of the concentration gradient. Finally, xylene could permeate though the membrane from feed side to vacuum side. A surface diffusion model fundamentally describes transport model in such dynamics. The theoretical model of a surface diffusion through microporous inorganic membranes was developed by Krishna et al.[36] based on Stefan-Maxwell theory. The model has been successfully used to predict the selectivity of hydrocarbon mixtures permeating through zeolite membranes using known properties of zeolites[19]. In this paper, we try to examine the fit of the surface diffusion model to the experimental binary and ternary mixture pervaporation data to gain a better understanding of the transport mechanism that occurs in cyclodextrin modified ceramic membranes.

For the estimation of flux using this mathematical model, the following assumption are made to compare with the pervaporation experiments:

1. The rate-determining process is the transport through the membrane. Mass transfer resistances in the liquid feed stream adjacent to the membrane and from the membrane to the vacuum region on the permeate side are neglected. The resistance of the flow through the support layer is also assumed to be small compared with that through the CD modified layer.
2. The adsorption of penetrants at both the feed and permeate sides of the membrane are assumed to be at equilibrium. The pressure on the permeate side in this study is zero.
3. Adsorption of xylenes in the CD modified membrane can be assumed to obey the Langmuir model.

First, the relationship of multicomponent permeation can be written in a generalized Fick's law form:

$$J_i = -\rho \sum_{k=1}^{s} D_{ik} \frac{\partial \theta_k}{\partial z}, i = 1,2,.....s \tag{14}$$

where J_i is the flux of penetrant i [m/s], ρ [kg/m^3] is the density of membrane, θ_i is the occupancy of penetrant i in the system, z is the distance into the membrane from the feed side, and D_{ik} is the multi component diffusion coefficient which has θ^2 components including the cross coefficients, $D_{ik,}$ can be described using Stefan-Maxwell theory[37].

Binary mixtures: For binary mixtures, the solution of Eq. (14) for the multicomponent diffusion coefficient can be described by Stefan-Maxwell theory[37]. In the permeation of xylenes through CD modified membranes considered here, the saturation loading for xylene isomers are the same, then the fluxes for species 1 and 2 can be transformed to the form of a deviation of occupancy to be solved numerically:

$$\frac{d\theta_1}{dz} = -\frac{J_1\left(1 + \theta_2 \frac{D_{11}}{D_{12}} + \theta_1 \frac{D_{22}}{D_{12}}\right)}{\rho q_m D_{11}\left[\left\{\Gamma_{11} + \theta_1 \frac{D_{22}}{D_{12}}\left(\Gamma_{11} + \Gamma_{21}\right)\right\} + \left\{\Gamma_{12} + \theta_1 \frac{D_{22}}{D_{12}}\left(\Gamma_{12} + \Gamma_{22}\right)\right\} X^{-1}\right]} \tag{15}$$

$$\frac{d\theta_2}{dz} = -\frac{J_2\left(1+\theta_2\frac{D_{11}}{D_{12}}+\theta_1\frac{D_{22}}{D_{12}}\right)}{\rho q_m D_{22}\left[\left\{\Gamma_{22}+\theta_2\frac{D_{11}}{D_{12}}\left(\Gamma_{22}+\Gamma_{12}\right)\right\}+\left\{\Gamma_{21}+\theta_2\frac{D_{11}}{D_{12}}\left(\Gamma_{21}+\Gamma_{11}\right)\right\}X\right]} \tag{16}$$

where X is given as follows:

$$X = \left(\frac{\left\{\Gamma_{22}+\theta_2\frac{D_{11}}{D_{12}}\left(\Gamma_{22}+\Gamma_{12}\right)\right\}-\frac{D_{11}J_2}{D_{22}J_1}\left\{\Gamma_{11}+\theta_1\frac{D_{22}}{D_{12}}\left(\Gamma_{11}+\Gamma_{21}\right)\right\}}{\frac{D_{11}J_2}{D_{22}J_1}\left\{\Gamma_{12}+\theta_1\frac{D_{22}}{D_{12}}\left(\Gamma_{12}+\Gamma_{22}\right)\right\}-\left\{\Gamma_{21}+\theta_2\frac{D_{11}}{D_{12}}\left(\Gamma_{21}+\Gamma_{11}\right)\right\}}\right) \tag{17}$$

and the elements of $[\Gamma]$ are given by the following equation:

$$\Gamma_{ij} = \left(\frac{q_{jm}}{q_{im}}\right)\frac{q_i}{p_i}\frac{\partial p_i}{\partial q_j}, i, j = 1, s. \tag{18}$$

where D_{ij} and D_{ii} are the Stefan-Maxwell diffusion coefficients, q_{im} is the saturation adsorption of the species i, q_i is the amount of adsorption of species i, s is the number of components and p_i is the pressure of species i. Occupancy, θ_i, is equal to q_i / q_{im}.

If adsorption equilibrium in the membrane is assumed to follow a Langmuir-type adsorption isotherm, equations (15) and (16) can be used to estimate the fluxes using only the sorption equilibrium on the feed side and the thermal intrinsic diffusivities in the membrane. The diffusivities are obtained from experiment and molecular simulation techniques, respectively.

If we use the adsorption isotherm of CD powder for the estimation of Eq. (18), the membrane density, ρ, can be written as:

$$\rho = \rho_{CD}\mu^* \tag{19}$$

where ρ_{CD} is the bulk density of β-CD and μ^* is the geometric factor related to the porosity and the condition of the polymerized CD layer.

Ternary mixtures: For a ternary mixture, Eq. (14) can be simplified by assuming that the Stefan-Maxwell coefficient, D_{ij}, is infinity. This assumption means that there are no interactions between the permeating species. Such condition is sometimes observed in the permeation of hydrocarbon molecules through MFI-type silicalite membranes[19, 38] where the interaction

between permeating molecules can be ignored because the interaction between the permeating molecules and the zeolite wall is larger than that between the penetrants. Also, the penetrants cannot pass each other due to their similar size to the pore. The validity of this assumption in our system will be discussed in a later section below. If we use this assumption, the form of a deviation of occupancy can be described as follows:

$$\frac{d\theta_1}{dz} = \frac{\Gamma_{12}\dfrac{\Gamma_{23}Y_1 - \Gamma_{13}Y_2}{\Gamma_{23}\Gamma_{12} - \Gamma_{13}\Gamma_{22}} + \Gamma_{13}\dfrac{\Gamma_{32}Y_1 - \Gamma_{12}Y_3}{\Gamma_{13}\Gamma_{32} - \Gamma_{12}\Gamma_{33}} - Y_1}{\Gamma_{12}\dfrac{\Gamma_{23}\Gamma_{11} - \Gamma_{13}\Gamma_{21}}{\Gamma_{23}\Gamma_{12} - \Gamma_{13}\Gamma_{22}} + \Gamma_{13}\dfrac{\Gamma_{32}\Gamma_{11} - \Gamma_{12}\Gamma_{31}}{\Gamma_{13}\Gamma_{32} - \Gamma_{12}\Gamma_{33}} - \Gamma_{11}} \tag{20}$$

$$\frac{d\theta_2}{dz} = \frac{\Gamma_{21}\dfrac{\Gamma_{23}Y_1 - \Gamma_{13}Y_2}{\Gamma_{23}\Gamma_{11} - \Gamma_{13}\Gamma_{21}} + \Gamma_{23}\dfrac{\Gamma_{31}Y_2 - \Gamma_{21}Y_3}{\Gamma_{31}\Gamma_{23} - \Gamma_{21}\Gamma_{33}} - Y_2}{\Gamma_{21}\dfrac{\Gamma_{23}\Gamma_{12} - \Gamma_{13}\Gamma_{22}}{\Gamma_{23}\Gamma_{11} - \Gamma_{13}\Gamma_{21}} + \Gamma_{23}\dfrac{\Gamma_{31}\Gamma_{22} - \Gamma_{21}\Gamma_{32}}{\Gamma_{31}\Gamma_{23} - \Gamma_{21}\Gamma_{33}} - \Gamma_{22}} \tag{21}$$

$$\frac{d\theta_3}{dz} = \frac{\Gamma_{31}\dfrac{\Gamma_{32}Y_1 - \Gamma_{12}Y_3}{\Gamma_{32}\Gamma_{11} - \Gamma_{12}\Gamma_{31}} + \Gamma_{32}\dfrac{\Gamma_{31}Y_2 - \Gamma_{21}Y_3}{\Gamma_{31}\Gamma_{22} - \Gamma_{21}\Gamma_{32}} - Y_3}{\Gamma_{31}\dfrac{\Gamma_{13}\Gamma_{32} - \Gamma_{12}\Gamma_{33}}{\Gamma_{32}\Gamma_{11} - \Gamma_{12}\Gamma_{31}} + \Gamma_{32}\dfrac{\Gamma_{31}\Gamma_{23} - \Gamma_{21}\Gamma_{33}}{\Gamma_{31}\Gamma_{22} - \Gamma_{21}\Gamma_{32}} - \Gamma_{33}} \tag{22}$$

where,

$$Y_i = \frac{-J_i}{\rho q_m D_{ii}}, i = 1,2,3 \tag{23}$$

By applying the multicomponent Langmuir equation to Eqs. (20)-(22), the fluxes and selectivity in ternary mixtures can be calculated.

Experimental: A T1-70 ceramic nanofilter from U.S. Filter Inc. having a molecular cut–off of 1000 roughly equivalent to 2 nm was used as a support. Figure 11 shows an SEM image of the cross-section of the support used. The top layer is porous TiO_2 (2 to 5 μm thick) and the second layer consists of a 20 μm layer of α-alumina. The third layer is α-alumina

consisting of the large particles compared to the particle size of the upper layers. A smooth and uniform surface is observed.

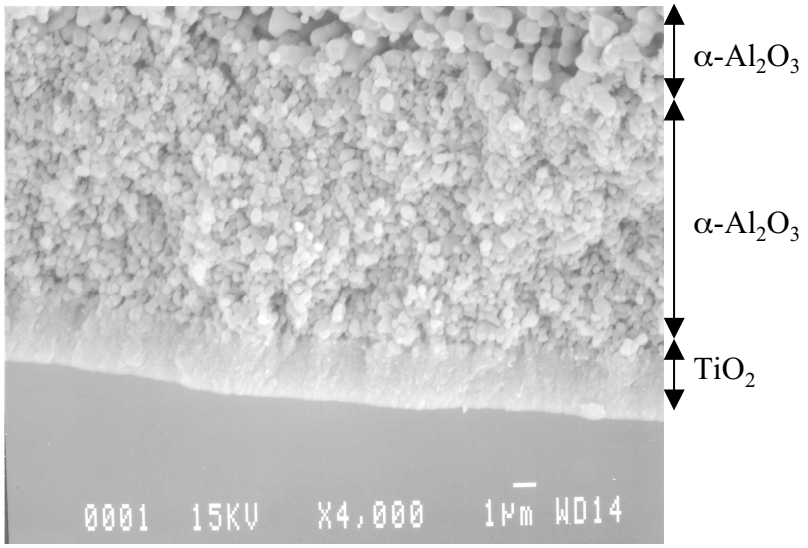

Figure 11. Cross-sectional view of the unmodified membrane used as support.

The ends of support were glazed to prevent axial flow in the support and were fired at 880 C for 20 minutes. Then the supports were cleaned by boiling them in aqueous hydrogen peroxide solution for 30 minutes. The tubes were also boiled in distilled water for 30 minutes to remove any residual hydrogen peroxide. After cleaning, the tubes were dried at 80 C for at least 5 hours in a vacuum oven.

A two step modification of the support by β-CD was carried out using the sodium type β-CD salt, the direct bonding method and the cross-linking method. The β-CD salt was prepared as follows. β-CD (11.5 g) was dried at 80 C overnight in a vacuum oven, and was dissolved in 175 mL of dimethylformamide (DMF) at room temperature with stirring. The solution was heated to 120 C and then 2 g NaH powder was added with stirring. After 5 minutes of heating, the solution was cooled down to 90 C, and then the sodium type β-CD salt solution was obtained. In the direct bonding method, a pre-treated ceramic tube was put into 100 mL of β-CD salt solution and was heated with stirring. The temperature and the reaction time in this procedure were subject to optimization. In order to cross-link the directly bonded β–CD modified alumina tube, the membrane was placed in 100 mL of dried toluene in a three-neck flask. The temperature was kept at 90 C and 2 g of Bis(trimethyl)octyl silane was added to the toluene solution and stirred for 15 minutes. Then, 60 mL of β–CD salt solution was added to the mixture and maintained at 90 C with stirring for 50 minutes. The membrane was washed with 100 mL of toluene and methanol, and then dried.

Bis(trimethyl)octyl silane was obtained from Petrarch Systems, HPLC grade DMF and NaH from Aldrich, toluene and methanol from Aldrich, de-ionized water and 30% hydrogen peroxide from Fisher Scientific were used in the synthesis.

Pervaporation Measurements . The pervaporation system for tubular membranes is shown schematically in Figure 12. The liquid feed is circulated between the membrane cell and a large feed vessel, which kept the feed stream at a constant composition. In the membrane cell, the active surface area of the tubular membrane, which is the inside surface, was 4.08 cm^2. The feed circulation rate was 0.238 L/min. The vacuum side was maintained less than 1 Pa using a mechanical vacuum pump and a vacuum controller (BUCHI B-720). Permeate samples are collected by the use of a liquid nitrogen cold trap. The total flux is determined from the amount of the permeate sample collected for a given time period. The permeate concentrations were analyzed by the use of a gas chromatograph (Hewlett Packard 6850A) equipped with a packed column (EC^{TM}-WAX, Alltech) and a mass-selective detector.

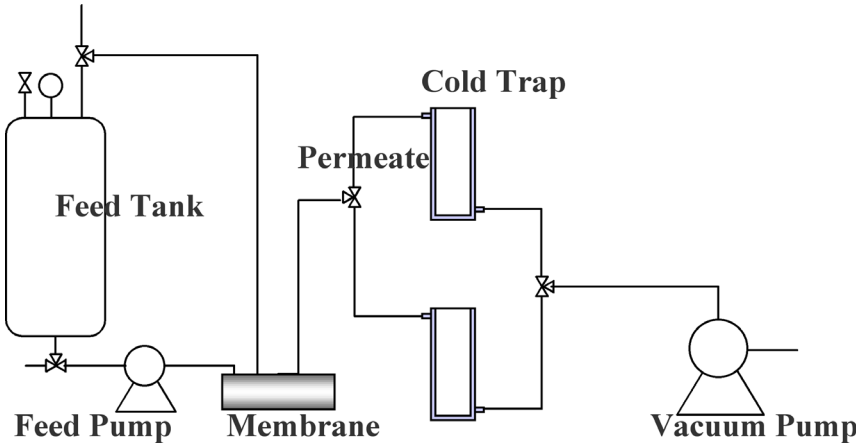

Figure 12. Schematic diagram of the apparatus used for the pervaporation tests.

The separation or concentration factor is determined using following equation:

$$S_{ij} = \frac{y_{ip} / y_{jp}}{y_{if} / y_{jf}} \tag{23}$$

where y_{if} is the concentration of species i on the feed side and y_{jp} is the concentration of species i on the permeate side.

Solubility of xylene isomers in β-cyclodextrin . Liquid phase adsorption isotherms of xylene isomers on β-CD powder were measured for the use as a parameter in the mathematical model. β-CD powder was dried at 80 °C in a vacuum oven overnight prior to the adsorption experiments. Xylene mixtures (20mL) were added to the dried β-CD powder (18 g) in a 125 mL flask. The flasks were tightly capped to prevent losses due to evaporation and were stirred for at least 6 hours using a shaker water bath at a constant temperature of 21 C. We confirmed that 6 hours is enough time to reach equilibrium. After that, 50 mL of ethyl alcohol was added to

extract the remaining xylenes that had not adsorbed in the CD cavity, then the flask was shaken for 1 hour. After waiting 30 minutes to settle the CD powder to the bottom of the flask, the liquid phase concentration is measured using a gas chromatograph. The amount of adsorption was estimated from the change of concentration of xylene in liquid phase by comparing with that of the blank.

Molecular Simulations: NVE ensemble (the number of atoms, volume and total energy are constant) molecular dynamics (MD) simulations were carried out to obtain the corrected diffusivity of xylenes through the CD modified membrane. Cerius2 version 4.0 code, purchased from Accelerys Inc, was used to perform the MD simulations. We chose the pcff 3.01 force field set for representing the inter and intra atomic interactions[39]. Interactions considered in this forcefield include bonding, angle, torsion, inversion, van der Waals, and electrostatic forces. The Ewald method was used for the summation of the electrostatic interactions. The interaction cutoff length for the van der Waals interactions was 9 Å. All atoms were allowed to move during the simulations. A velocity corresponding to the Boltzmann distribution at 260 K-294 K was given to all atoms in an MD unit cell before performing the MD calculations. The average temperature after 100 ps for all simulations was confirmed to be 294 K ± 7 K. 500ps MD runs were performed with the time step 1 fs and the last 400 ps trajectories of atoms were used for estimating the self-diffusion coefficients, which were calculated by the mean square displacement of each atom of the xylene molecules with an average over 2 ps of time using the Einstein relationship.

Results and Discussion:

Optimization of Membrane Synthesis Conditions and Characterization: In order to achieve a high selectivity and flux, our objectives were to synthesize a CD modified membrane having a smooth, defect-free surface with the minimum membrane thickness. Hence, we examined the effect of the reaction time and temperature of the direct bonding method on the surface morphology using scanning electron microscopy (SEM, JEOL JXA-840). The temperatures investigated were 110 C and 120 C and the reaction times investigated were 40 minutes, 80 minutes and 110 minutes. We have confirmed that temperature higher than 120 C causes the rapid formation of polymerized CDs in the solution and makes the membrane surface rough. In these experiments, we used small pieces of the ceramic membrane in the reaction that is carefully broken into small species. The modified pieces are dried in the oven at 50 C before SEM observation. SEM images of the membranes are presented in Figures 13 and 14. In Figure 13, the reaction temperature was 110 C, and cracks are observed on the membrane surface for the 40 minute and 80 minute reaction times. As the reaction time was increased, the surface was covered with the CD phase, and finally, CD particles were deposited after 110 minutes of reaction time. On the other hand, in Figure 14, the support surfaces were completely covered with the CD phase in 40 minutes reaction time, although the cracks in the CD layer were observed. As the reaction temperature was increased to 120 C, a sticky crystalline layer of CD particles appeared on the surface. From these images, it seems that the optimal reaction temperature and reaction time are 120 C and around 40 minutes, respectively. However, it was difficult to obtain a crack-free membrane using the direct bonding method.

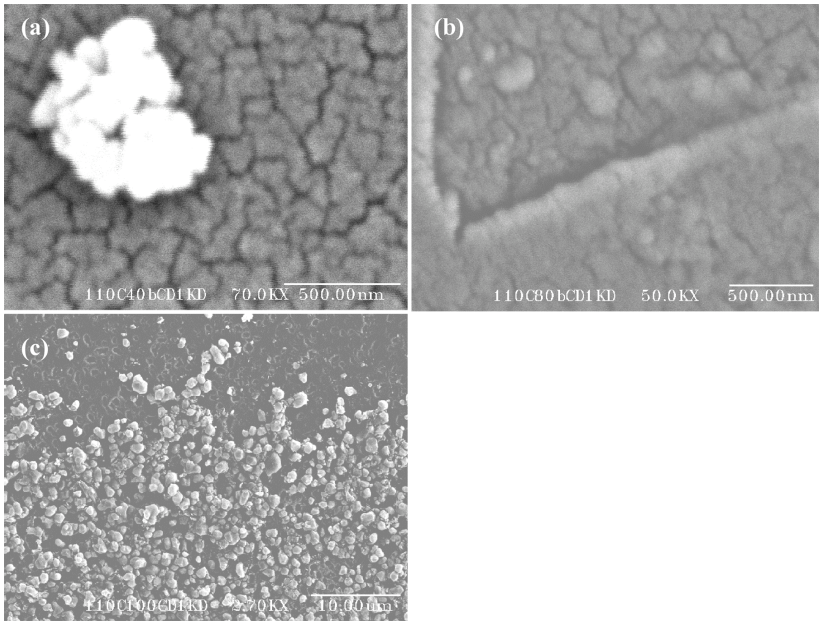

Figure 13. SEM images showing the influence of reaction time on the membrane surface structure using the direct bonding method at 110 C. The reaction times are (a) 40 minutes, (b) 80 minutes, and (c) 110 minutes. Magnification levels are 70000, 50000 and 27000 times, respectively.

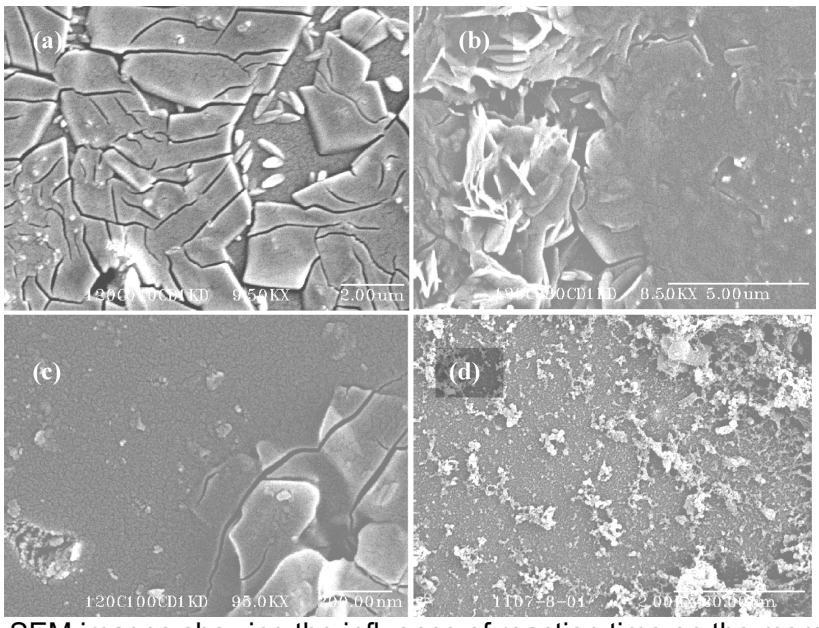

Figure 14 (a)-(c) SEM images showing the influence of reaction time on the membrane surface structure using the direct bonding method at 120 C. The reaction times are (a) 40 minutes, (b) 80 minutes, and (c) 110 minutes. (d) SEM image of the surface of a cross-linked β-CD modified membrane. Magnification levels are 9500, 8500, 9500 and 2000 times, respectively.

Better results were obtained by cross linking the CD layer after the direct bonding synthesis method. Figure 14(d) shows the surface of a cross-linked membrane. There were no cracks observed on the surface. The reaction conditions for the direct bonding method were a temperature of 120 C and a reaction time of 40 minutes. It is noted that the cross-linking method should be carried out immediately after the direct bonding method, otherwise the CD layer will crack. Figure 15 is an image of a cross-section of a cross linked membrane. From Figure 15, the thickness of the CD layer could not identified on the top layer of the membrane, suggesting that the CD layer penetrated into the ceramic support. Comparing Figure 15 with the SEM image of an unmodified membrane shown in Figure 11, the impregnated CD layer seems to reach at the second layer of α-Al_2O_3 and that thickness can be estimated to be about 24 μm.

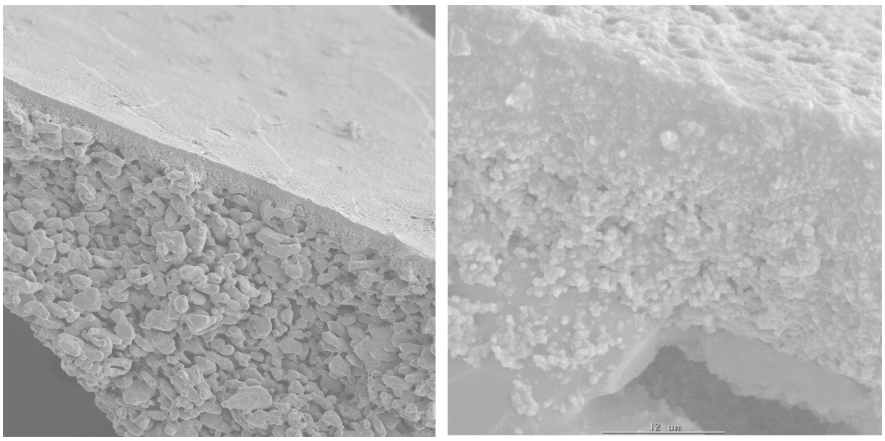

Figure 15. SEM images of the surface and cross-section of a cross-linked β-CD modified membrane. Magnification levels are (right) 200 and (left) 2000 times.

The pore size of the top layer is approximately 2 nm and that is close to the molecular size of a CD molecule, but there might be room for the cross linker molecules to diffuse through the CD layer because of the presence of a pore size distribution in the top layer. Furthermore, the CD and cross linker can also diffuse from the backside of asymmetric membranes. Hence, the cross-linked CD would be structured to fill the pore or coat on the pore wall in the larger pore layer.

Pervaporation Results: Pervaporation of ternary mixtures using non-modified membrane is carried out to examine the intrinsic selectivity of support. The unmodified membrane showed much higher flux of about 146 kg/m^2/hr than the CD modified membrane and no selectivity beyond that from vapor liquid equilibrium was observed for any of the xylene isomers.

The pervaporation experiment for the ternary mixtures of xylene isomers was then carried out using the CD-modified ceramic membranes. The feed was an equivolume xylene ternary mixture. The selectivities measured were: *m*-/*p*-xylene of 1.39, *o*-/*p*-xylene of 1.33, and *m*-/*o*-xylene of 1.05, with a flux of 0.03 kg/m^2/hr. The order of flux is m- > o- > p-xylene.

The pervaporation results for *p*-/*m*-xylene binary mixtures are presented in Figure 16 as a function of the feed *p*-xylene concentration. The flux increases with an increase in the feed concentration of p-xylene. The dependency of the flux on the feed concentration also has been observed in CD containing polymeric membranes[24, 25]. The measured selectivity is a strong function of the *p*-xylene feed concentration. The selectivity decreased from 1.5 to 0.7 as the *p*-xylene concentration in the feed increases. A more detailed discussion about this will be presented in the section 5.4. The fastest penetrant at low *p*-xylene concentrations in the feed is *p*-xylene, and the selectivity gradually changes to the meta-selectivity as the *p*-xylene concentration in the feed increases.

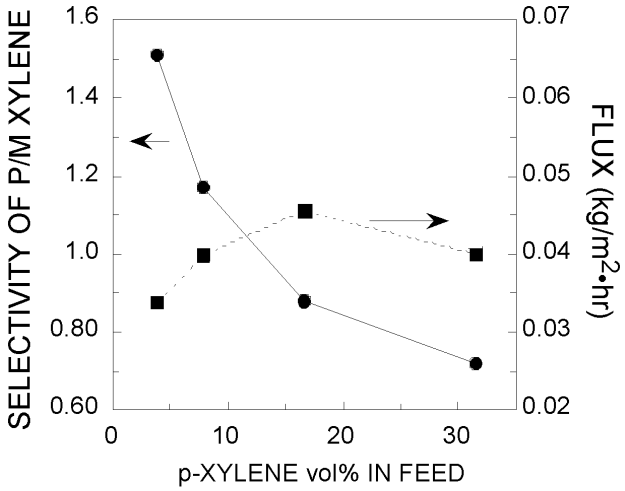

Figure 16. Pervaporation results for *p*-xylene/*m*-xylene binary mixtures as a function of *p*-xylene concentration in the feed.

Similar trends for the selectivity have been reported with polymeric membranes[24-26], although the penetrants were different with those investigated here. A PVA/β-CD membrane for the water/ethanol binary mixture separation has been reported to have a maximum selectivity at a feed ethanol concentration 50 wt%[6], while a PVA/β-CD membrane for the separation of *p*-/*m*-xylene binary mixtures has exhibited a maximum in selectivity when the p-xylene feed concentration was 10 wt%[26]. However, our membrane has no maximum in the selectivity like those polymeric membranes. The reported decline of the selectivity in polymeric membranes may be due to the contribution of a swelling effect. In our membrane, the CD was confined inside the pore and the swelling effect would be suppressed.

Molecular Simulation Results: To perform an MD simulation one needs information regarding the molecular configuration of CD in the membrane. The SEM image of a cross-sectional view of the CD modified membrane in Figure 15 shows that the CD phase filled the pores of the ceramic membrane. Since the pore size of top layer of the support membrane is close to the diameter of a CD molecule, CD molecules inside the pore were assumed to be densely packed so that their density will be close to the bulk density of pure CD. CD molecules in the pore might be connected each other by polymerization. However, in the molecular simulations, in order to simplify the unknown structure, the effect of a polymer network of cross-

linked CD molecules is assumed to be small and ignored. This assumption would be reasonable because the cross-linking procedure is performed after the impregnation procedure of CD. Therefore, we use the densely packed CD structure as the model for representing a CD layer of the membrane.

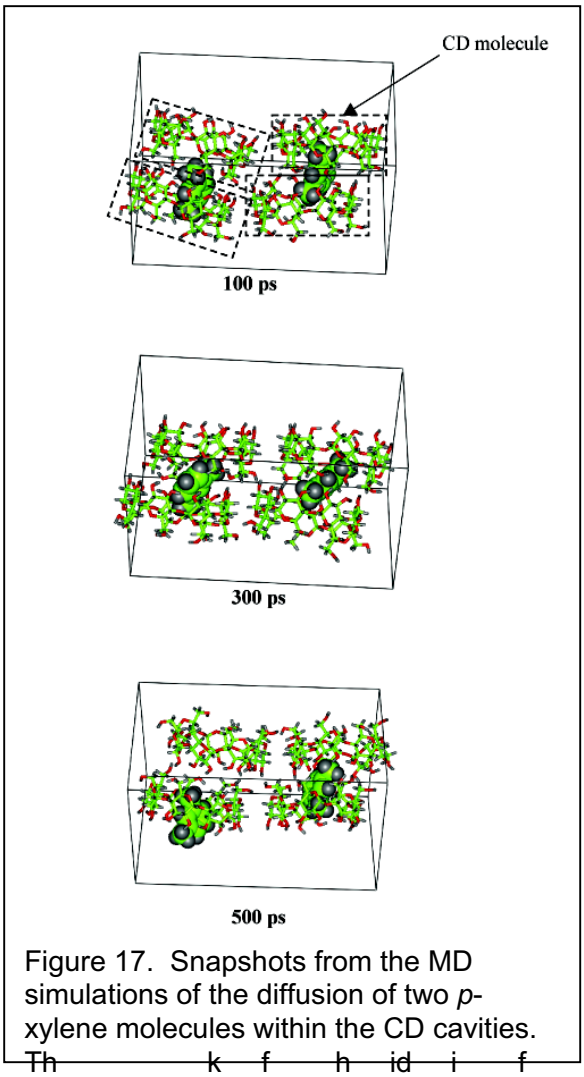

Figure 17. Snapshots from the MD simulations of the diffusion of two *p*-xylene molecules within the CD cavities.

The unit cell for the MD simulation contained 4 β-CD molecules and 2 xylene molecules, which are the same isomers, with the cell dimensions; a = 33.0 Å, b = 19.0 Å, and c = 20.0 Å. The density of CD is 0.6 g/cm^3, which corresponds to the density of the bulk CD; 0.4~0.7 g/cm^3. The configuration of molecules in the unit cell was energetically optimized using a molecular mechanics calculations before performing the MD simulations. Figure 17 shows snap shots of the unit cell during the MD simulations. As shown in this figure, four CD molecules in the unit cell are arranged so that their cavity openings are essentially the same direction, although after minimization two of the CDs are slightly inclined. Xylene molecules can diffuse thorough the cavity of two stacked CDs and it would be extremely difficult for them to jump to another path of a neighboring CD pair because there is not enough space for the xylene to fit between two stacked CDs. In this Figure, the diffusion of p-xylene molecules between two neighboring CDs is shown. This transport dynamic occurred 4~6 times during the MD simulation runs; xylene molecules remained almost the entire simulation period inside the cavity. This means that the movement of xylene molecules is likely to be diffusion by a hopping mechanism. Similar dynamics were also observed during the MD results with both m-xylene and o-xylene.

The Stefan-Maxwell diffusion coefficients we need for the mathematical model correspond to the self-diffusion coefficients that were obtained from the MD simulations only when the concentration of diffusing species is zero[40, 41]. In our MD simulations, the unit cell contains two diffusing molecules; the occupancy studied is not zero precisely. However, two xylene molecules in the unit cell are located separately with their own diffusional paths, and the interactions with the CD molecules were so large so that the interaction between the diffusing xylene molecules was neglected. Under such a condition, it would be a reasonable approximation that the calculated self-diffusion coefficients are the Stefan-Maxwell diffusion coefficients we need.

The estimated Stefan-Maxwell diffusion coefficients from the MD simulations are summarized in Table 5. The diffusion order is *m*- > *o*-> *p*-xylene. The diffusion coefficients obtained are about two orders lower than that of aromatic molecules in a benzene solvent, e.g. 1.35×10^{-9} m^2/s for toluene. This suggests that the strong interaction between the CD cavity and the xylenes molecules slows the diffusion of the xylenes.

Table 5. The Stefan-Maxwell diffusion coefficients of xylenes isomers in the CD phase obtained from MD simulations.

Solute	D_{ii} [$\times 10^{-11}$ m^2/s]
p-xylene	3.84
m-xylene	6.46
o-xylene	4.47

The heat of the formation of the inclusion complexes are calculated using molecular mechanics methods for the 1:1 and 1:2 (host: guest) complexes. The results are summarized in Table 6. The most energetically stable complex was chosen from the several initial configurations. The order of the inclusion complex strength is *o*- > *p*- > *m*-xylene which are consistent with the reported formation constants at 25 C in aqueous solution [42]. This order is opposite of the order of the estimated diffusion coefficients except *o*-xylene. This means that the interaction strength is fundamentally factored into the determination of their diffusion rate; however, the entropic effect is also an important factor on the diffusion rate. Actually, the most stable configuration for a *p*-xylene molecule indicates that two methyl groups interact with the cavity mouth. Such a configuration where the molecular axis tilts to the diffusion direction would reduce its diffusion rate.

Comparison between the mathematical model predictions and flux and selectivity measurements: The pervaporation results including the flux and selectivity were compared with those estimated by the mathematical model. The model parameters related to the membrane are summarized in Table 7. In this table, the density of CD, ρ_{CD}, is the same as that of the unit cell used in MD calculations. The membrane thickness was obtained from the SEM image (Figure 15) of the membrane cross section. The saturation amount of adsorption, q_m, was calculated assuming a 1:1 complex. The structural factor, μ^*, which mainly relates to the porosity of the membrane, is assumed 0.14. This value is smaller than the porosity of the support top layer which is 0.2 to 0.25. The parameter μ^* only effects the magnitude of flux. Figure 18 shows the adsorption isotherm of *p*-/*m*-xylene binary mixtures as a function of the feed p-xylene concentration. This adsorption isotherm is used for estimating the amount of adsorption on the feed side. The equations of the functions fit to these adsorption isotherms as a function of the feed p-xylene concentration are $Y = -7.61 \times 10^{-7} X^3 + 7.31 \times 10^{-5} X^2 + 0.010X$ for *p*-xylene and $Y = 8.56 \times 10^{-8} X^3 - 1.67 \times 10^{-5} X^2 - 9.13 \times 10^{-3} X + 1.016$ for *m*-xylene, with correlation coefficients (R^2) of 0.997 and 1.00. For the calculation of the D_{ij} we employed three approximations; D_{ij} is infinity (the terms containing D_{ij} in the denominator vanish numerically), and the simple average of the diffusion coefficient of two components given by:

$$D_{ij} = 0.5(D_{11}+D_{22}) \quad (25)$$

Table 6. The inclusion energies for xylene isomers in a β-CD cavity estimated by molecular mechanics calculations. 1:1 2:1 (guest:host) complexes were assumed. The unit is kcal/complex. E (inclusion energy) was estimated from the total energy differences before and after the formation of the inclusion complex: E(host) + E(guest) – E(complex). The adsorption energies on the torus (outside) of the CD imply no selectivity for the outside of CD cavity.

Guest species	Number of guests	β-CD	
		Inside	Torus
p-xylene	1	18.4	9.9
o-xylene	1	19.8	10.0
m-xylene	1	17.3	9.4
p-xylene	2	27.9	-
o-xylene	2	17.2	-
m-xylene	2	27.2	-

Table 7. The parameters used in the mathematical model.

ρ_{CD} [kg/m^3]	μ^* [–]	L [μm]	q_m [kg-xylene/kg-CD]
601.4	0.08	24	0.0846

and the Vignes correlation as proposed by Krishna[43] is as follows:

$$D_{ij} = D_{11}^{\theta 1/(\theta 1+\theta 2)} D_{22}^{\theta 2/(\theta 1+\theta 2)} \quad (26)$$

The simple average of D_{ij} does not depend on the adsorption isotherm, while the Vignes equation depends on it.

Figure 19 represents the comparison of the selectivity of the model predictions with the experimental results as a function of the feed *p*-xylene concentration. As shown in this Figure, the calculated values assuming D_{ij} = infinity have the best fit with the experiments. In the predictions using a non-zero D_{ij} in the mathematical model, the selectivity declines slightly at low *p*-xylene concentration in the feed. The fit with the line when D_{ij} equals infinity implies that the 1:1 complex formation is dominant in the membrane. This speculation is supported by the inclusion strength data where the 1:1 complex is more stable than the 1:2 (host: guest) complex as shown in Table 6. Figure 20 shows the comparison of the flux predicted by the mathematical model with the experiments. The experimental fluxes are well predicted by the mathematical model provided that D_{ij} is infinity. It should be noted that the flux change with an increase in the feed concentration is also predicted in the mathematical model. The agreement of the pervaporation results with those predicted by the mathematical model indicates that the

transport mechanism in this membrane is likely controlled by a surface diffusion mechanism, and that the terms containing D_{ij} could be neglected in our system.

The selectivity of the pervaporation process is basically a function of the sorption equilibrium and the diffusion rates in the membrane. To provide a better understanding of the factors that control the transport, two sets of model calculations were carried out. In the first calculation, Model 1, the individual diffusivities for two isomers are assumed to be equal to examine the effect of the solubility difference. In another calculation, Model 2, it is assumed that the individual solubility ratio of the isomers on the feed side is equal to the ratio of the feed concentrations while the diffusivity differences are considered independently. Predicted flux and selectivity for these models are presented in Figures 21 and 22, respectively. As shown in these figures, the trends of flex and selectivity between two models are similar, and the best fit with the change of the selectivity of the experimental data is that of Model 2. This suggests that the strong dependency of the selectivity on the feed concentration is mainly due to the contributions from the differences in the diffusion rates.

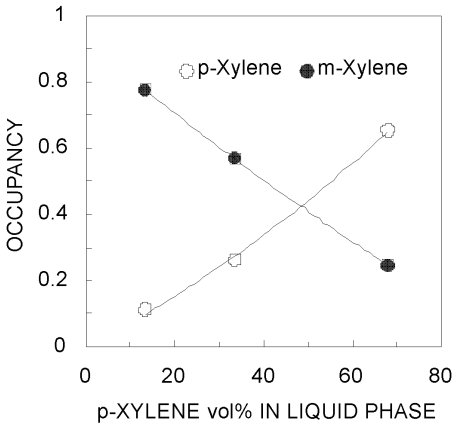

Figure 18. Sorption isotherms for the *p*-/*m*-xylene binary system.

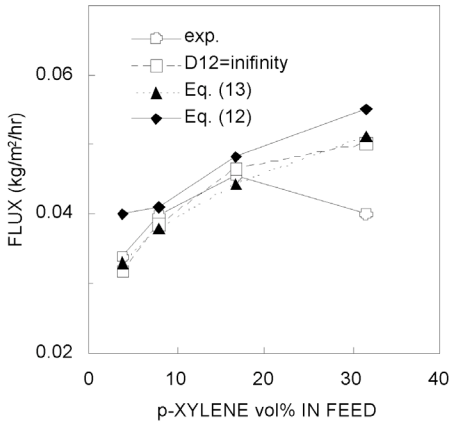

Figure 19. Comparison of the predicted fluxes and the experimental results for the *p*-/*m*-xylene binary mixtures. Predictions using three approximations for D_{ij} are shown.

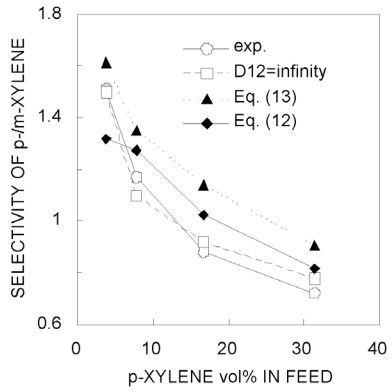

Figure 20. Comparison of the predicted selectivities and the experimental results for the *p*-/*m*-xylene binary mixtures. Predictions using three approximations of D_{ij} are shown.

The selectivity of the pervaporation process is basically a function of the sorption equilibrium and the diffusion rates in the membrane. To provide a better understanding of the factors that control the transport, two sets of model calculations were carried out. In the first calculation, Model 1, the individual diffusivities for two isomers are assumed to be equal to examine the effect of the solubility difference. In another calculation, Model 2, it is assumed that the individual solubility ratio of the isomers on the feed side is equal to the ratio of the feed concentrations while the diffusivity differences are considered independently. Predicted flux and selectivity for these models are presented in Figures 21 and 22, respectively. As shown in these figures, the trends of flex and selectivity between two models are similar, and the best fit with the change of the selectivity of the experimental data is that of Model 2. This suggests that the strong dependency of the selectivity on the feed concentration is mainly due to the contributions from the differences in the diffusion rates.

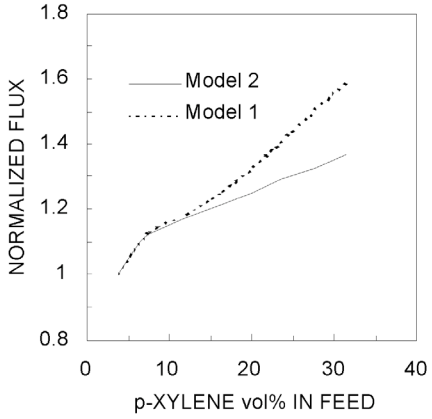

Figure 21. Predicted changes of the fluxes in the two models as a function of the feed *p*-xylene concentration. Model 1 assumed that the diffusion coefficients for two components are equal while the sorption parameters are correctly considered. Model 2 assumed that the sorption occupancy on the feed side is the same as the ratio of the feed concentrations, while the diffusivities are correctly considered.

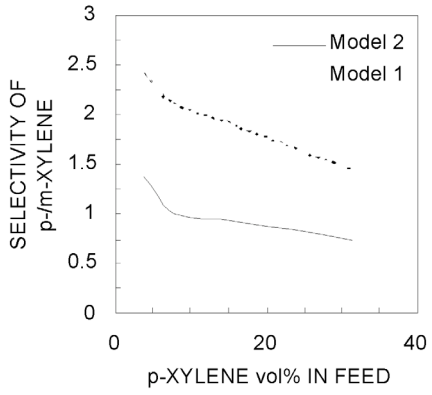

Figure 22. Predicted changes of the selectivity in the two models as a function of the feed *p*-xylene concentration. See Figure 21 for the explanation of the assumptions in Models 1 and 2.

Table 8 compares the prediction of the selectivity and flux with the experiments data for ternary mixtures. Feeds are equivolume ternary mixtures. The equilibrium amount of sorption on the feed side used in the mathematical model is obtained from a sorption test for a ternary mixture. The results are 0.033 kg-p-xylene/kg-CD, 0.025 kg-m-xylene/kg-CD, and 0.035 kg-o-xylene/kg-CD. The predicted order of the flux is m->o->p-xylene with the flux of 0.03 kg/m^2/hr, and those are in good agreement with the experiments. This suggests that the pervaporation of the ternary mixtures is also explained well by our Stefan-Maxwell based surface diffusion model.

The MD simulation indicated the order of the selectivity predicted from the diffusion coefficents of xylene isomers in CD is m- > o- > p-xylene. On the other hand, the order from the sorption measurements is o- > p- > m-xylene. Indeed, the relationship between the selectivity and the diffusivity and solubility is almost opposite. This means that the selectivity based on the solubility difference is compensated by that based on the diffusivity. However, the effect of the diffusivity differences overcomes the solubility differences, especially at the lower concentrations, as shown in the pervaporation data.

Table 8. Comparison of the flux and selectivity of the pervaporation experiments with the values predicted using the mathematical model. $\mu^* = 0.08$.

	Total flux [kg/m^2/hr]	Selectivity		
		m-/*p*-xylene	*o*-/*p*-xylene	*m*-/*o*-xylene
experiment	0.03	1.39	1.33	1.05
calculation	0.03	1.28	1.23	1.04

Conclusions: Cyclodextrin (CD) modified ceramic membranes for the separation of mixtures of xylene isomers were fabricated using a direct attachment method using CD salt solutions. The CD layer formed was further stabilized using a cross-linking procedure. SEM images revealed that the CD layer penetrated into the ceramic membrane support to a depth of about 24 μm. Pervaporation tests using this membrane showed that the order of permeation from ternary xylene mixtures was *m*-xylene > *o*-xylene > *p*-xylene. In *p*- /*m*-xylene binary mixtures, the separation was a strong function of the feed concentration ratio. The selectivity decreased from 1.52 to 0.72 as the feed p-xylene concentration increased from 4 volume % to 32 volume %. The flux increased as the feed concentration increased and the maximum value was about 0.05 kg/m^2/s. A mathematical model based on Stefan-Maxwell theory assuming a surface diffusion mechanism was derived to explain the pervaporation results. Using the model parameters obtained from liquid phase adsorption tests and MD simulations, predictions of the selectivity and flux were in good agreement with the pervaporation results for both *p*-/*m*-xylene binary and *p*-/*m*-/*o*-xylene ternary mixtures. This consistency supports our hypothesis that the separation mechanism in the CD modified membrane is based on surface diffusion. Model calculations indicated a strong dependence of the selectivity on the feed concentration is presumably due to differences in the diffusion rate. The successful description of the performance of the CD modified membrane based on the mathematical model, whose required parameters that can be obtained from simple sorption tests and molecular simulations, will be helpful for the prediction of unknown selectivity of particular separation systems.

Nomenclature:

A	[m^2]	membrane area
a	[Π]	activity
$c_{i0,m}$	[kg/m^3]	concentration of *i* at position 0
$c_{iL,m}$	[kg/m^3]	concentration of species *i* at position L.
D_i	[m^2/s]	diffusion coefficient of species *i*
E_{coh}	[MJ]	cohesive energy
J_i	[kg/m^2 s]	flux of species *i*
K_i^{gas}	[kg/m^3 Pa]	gas phase sorption coefficient
L	[μm]	membrane thickness
p_{i0}	[Pa]	partial pressures of species *i* in equilibrium with $c_{i0,m}$
p_{iL}	[Pa]	partial pressures of species *i* in equilibrium with $c_{i0,L}$
P_i	[(m^2/s)(kg/m^3 Pa)	permeability of species *i*; the product of D_i and K_i^{gas}.
q	[kg]	mass of permeate
Q	[kg μm/m^2 hr.]	permeation rate / normalized flux
t	[hr. / s]	time
T	[C]	temperature
V	[m^3]	volume
$w_{P,i}$	[Π]	weight fraction of component *i* in permeate
$w_{F,i}$	[Π]	weight fraction of component *i* in feed.
W_d / W_s	[g]	weight of dry sample / weight of swollen sample
α	[Π]	separation factor
Γ_k	[Π]	group residual activity
Γ^j_k	[Π]	group residual activity in a reference solution of pure *j*.
δ	[$MPa^{1/2}$]	solubility parameter
φ_i	[Π]	volume fraction of species *i*
μ	[J/kg mol]	chemical potential
$\tilde{\nu}$	[Π]	reduced volume fraction
ν^j_k	[Π]	number of groups of type *k* in molecule *j*
ΔH_{VAP}	[MJ]	enthalpy of evaporation
$3c_1$	[Π]	number of external degrees of freedom per molecule

Patents:

A patent was filed on 1/25/03 describing the rubbery blend membranes and applications using them to separate aromatic hydrocarbons from aliphatic hydrocarbons as well as the separation of acid gases and nitrogen from methane. The title of the patent is: POLYMER BLENDS AND METHODS OF SEPARATION USING THE SAME.

Publications/Presentations:

Nam, S.Y. and J.R. Dorgan, 2002 North American Membrane Society Annual Meeting, Los Angeles, CA, 5/02, Tuning Pervaporation Membrane Performance through Rubbery Blends: Application to Benzene-Cyclohexane Separation.

Takaba, H. and J. D. Way, 2002 North American Membrane Society Annual Meeting, Los Angeles, CA, 5/02, Separation of Isomeric Xylenes using Cyclodextrin Modified Membranes

Takaba, H. and J. D. Way, "Separation of Isomeric Xylenes Using Cyclodextrin Modified Ceramic Membranes," *I&EC Res.*, *I&EC Res.*, **42**(6), 1243–1252(2003).

Stone, M.L., Orme, C.J., Stewart, F.F., Benson, M.T. and Peterson, E.S., "Gas Permeation Characteristics of Four Fluorinated Polymers", *Amer. Chem. Soc. Polymer Preprints* **2002**, *43(2)*, 1374

Orme, C., Stewart, F. and Stone, M. "Gas Transport Properties of Designer Phosphazene Polymers", 2002 North American Membrane Society Annual Meeting, Los Angeles, CA, 5/02.

Christopher J. Orme, John R. Klaehn, and Frederick F. Stewart, "Gas Permeability of Polyphosphazenes Bearing Substituted Aromatic Pendant Groups" Manuscript in Preparation for Submission to *J. Membr. Sci.*

Nam, S.Y. and J.R. Dorgan, *A priori design of solubility selective membranes. J. Memb. Sci.*, 2002. In Preparation.

References:

1. U. S. DOE, *1994 Manufacturing Energy Consumption Survey*. 1997.
2. Fleming, H.L., *Dehydration of organic / aqueous mixtures by membrane pervaporation.* Proc. Int. Conf. on Fuel Alcohols and Chemicals, 1989.
3. Baker, R.W., E.L. Cussler, W. Eykamp, W.J. Koros, R.L. Riley, and H. Strathmann, *Membrane Separations Systems - A R&D Needs Assessment*. 1990.
4. Ho, W.S.W. and K.K. Sirkar, eds. *Membrane Handbook*. 1992, VanNostrand Reinhold: New York.
5. Ho, W.S.W. and K.K. Sirkar, *Membrane Handbook*. 1992, New York: VanNostrand Reinhold.
6. Schell, W.J., C.D. Houston, and W.L. Hopper, *Membranes can efficiently separate carbon dioxide from mixtures.* Oil Gas Journal, 1983. **81**(33): p. 52-56.
7. Stephan, W., R.D. Noble, and C.A. Koval, *Design Methodology for a Membrane / Distillation Hybrid Process.* Journal of Membrane Science, 1995. **99**: p. 259.
8. Rautenbach, R. and R. Albrecht, *The Separation Potential of Pervaporation Part 2. Process Design and Economics.* Journal of Membrane Science, 1985. **25**: p. 25-54.
9. White, L.S., *Transport Properties of a polyimide solvent resistant nanofiltration membrane.* J. Memb. Sci., 2002. **205**: p. 191-202.
10. Hofmann, W., *Rubber Technology Handbook*. 1980, Munich: Hanser.
11. Wijmans, J.G. and R.W. Baker, *The Solution-Diffusion Model: A Review,.* Journal of Membrane Science, 1995. **107**: p. 1.
12. Sperling, L.H., *Introduction to Physical Polymer Science*. 3rd ed. 2001, New York: John Wiley and Sons.

13. Hansen, C.M., *Hansen Solubility Parameters: A User's Handbook*. 2000, Boca Raton, FL: CRC Press.
14. Oishi, T. and J. Prausnitz, *Estimation of Solvent Activities in Polymer Solutions Using a Group-Contribution Method.* Ind. Eng. Chem. Process Des. Dev., 1978. **17**(3): p. 333-339.
15. Nam, S.Y. and J.R. Dorgan, *A priori design of solubility selective membranes.* J. Memb. Sci., 2002. **In Preparation**.
16. Amerongen, G.J.v., *The Permeability Of Different Rubbers To Gases And Its Relationship To Diffusivity And Solubility.* Journal of Applied Physics, 1946. **17**: p. 972.
17. Barrer, R.M., *Permeation, Diffusion, And Solution Of Gases In Organic Polymers.* Transactions of the Faraday Society, 1939. **35**: p. 628.
18. Orme, C.J., M.K. Harrup, T.A. Luther, R.P. Lash, K.S. Houston, D.H. Weinkauf, and F.F. Stewart, *Characterization of gas transport in selected rubbery amorphous polyphosphazene membranes.* Journal of Membrane Science, 2001. **186**(2): p. 249-256.
19. Baertsch, C.D.F., H. H.; Falconer, J. L .; Noble R., *Permeation of Aromatics Hydrocarbon Vapors through Silicalite-Zeolite Membranes.* J. Phys. Chem., 1996. **100**: p. 7676.
20. Xomeritakis, G.L., Z.; Tsapatis, M., *Separation of Xylene isomers Vapors with Oriented MFI Membranes Made by Seeded Growth.* Ind. Eng. Chem. Res., 2001. **40**: p. 544.
21. Wegner, K.D., J.; Lin, Y. S., *Polycrystalline MFI Zeolite Membranes: Xylene Pervaporation and its Implication on Membrane Microstructure.* J. Membr. Sci., 1999. **158**: p. 17.
22. Wytcherley, R.W.M., F. P., *The Separation of meta- and para-Xylene by Pervaporation in the Presence of CBr4 a Selective Feed-Complexing Agent.* . J. Membr. Sci., 1992. **67**: p. 67.
23. Mulder, M.H.V., *Separation of Isomeric Xylenes by Permeation in Cellulose Ester Membranes.* J. Membr. Sci., 1982. **11**: p. 349.
24. Yamasaki, A.I., T.; Masuoka, T.; Mizoguchi, K., *Pervaporation of Ethanol/Water through a Poly(Vinyl Alcohol)/Cyclodextrin (PVA/CD) Membrane.* J. Membr. Sci., 1994. **89**: p. 111.
25. Chen, H.L.W., L. G.; Tan, J.; Zhu, C. L., *PVA Membrane Filled b-Cyclodextrin for Separation of Isomeric Xylenes by Pervaporation.* Chem. Eng. J., 2000. **78**: p. 159.
26. Miyata, T.I., T.; Uragami, T., *Characteristics of Permeation and Separation of Xylene Isomers through Poly (Vinyl Alcohol) Membranes Containing Cyclodextrin.* Macromol. Chem. Phys., 1996. **197**: p. 2909.
27. Krieg, H.M.B., J. C.; Keizer, K., *Chiral Resolution by b-Cyclodextrin Polymer-impregnated Ceramic Membranes.* . J. Membr. Sci., 2000. **164**: p. 177.
28. Sikonia, J.G.M., F. P., *Separation of Isomeric Xylenes by Permeation through Modified Plastic Films.* J. Membr. Sci., 1978. **4**: p. 229.
29. Krieg, H.M.L., J.; Keizer, K.; Breytenbach, J. C., *Enrichment of Chlorthalodone Enantiomers by Aqueous Bulk Liquid Membrane Containing β-Cyclodextrin.* J. Membr. Sci., 2000. **167**: p. 33.
30. Lue, S.J.J., H. J.; Hou, S. Y., *Permeation of Xylene isomers through Supported Liquid Membranes Containing Cyclodextrins.* Sep. Sci. Technol., 2002. **37**: p. 463.
31. Rekharsky, M.V.I., Y., *Complexation Thermodynamics of Cyclodextrins.* Chem. Rev., 1998. **98**: p. 1875.

32. Armstrong, D.W.D., W.; Alak, A.; Hinze, T. E.; Bui, K.H., *Liquid Chromatography Separation of Diastereomers and Structural Isomers on Cyclodextrin-Bonded Phases.* Anal. Chem., 1985. **57**: p. 234.
33. Ching, C.B.H., K.; Liu, X., *Sorption and Diffusion of Cresols on Bonded b-Cyclodextrin-Silica Stationary Phase.* Ind. Eng. Chem. Res., 1993. **32**: p. 2789.
34. Davies, J.E.D.K., W.; Powell, H. M.; Smith, N. O., J. Incl. Phenom., 1983. **1**: p. 3.
35. Uematsu, I.J., *Selective Liquid-Liquid Extraction of Xylene Isomers and Ethylbenzene though Inclusion by Branched a-Cyclodextrin.* Incl. Phenom. Mol. Recog. Chem., 1992. **13**: p. 1.
36. Krishna, R., *Multicomponent Surface Diffusion of Adsorbed Species. A Description Based in the Generalized Maxwell-Stefan Diffusion Equations.* Chem. Eng. Sci., 1990. **45**: p. 1779.
37. Kapteijn, F.M., J. A.; Krishna, R., *The Generalized Maxwell-Stefan Model for Diffusion in Zeolites: Sorbate Molecules with Different Saturation Loadings.* Chem. Eng. Sci., 2000. **55**: p. 2923.
38. van den Broeck, L.J.P.B., W. J. W.; Kapteijn, F.; Moulijin, J. A., *Binary Permeation through a Silicalite-1 Membrane.* AIChE J., 1999. **45**: p. 976.
39. Molecular Simulations, I., *Cerius2 Software Manual*. 1997, Molecular Simulations, Inc.: San Diego.
40. Karger, J.R., D. M., *Diffusion in Zeolite and Microporous Solids*. 1992, New York: Wiley-Interscience.
41. Suzuki, S.T., H.; Yamaguchi, T.; Nakao, S., *Estimation of Gas Permeability of a Zeolite Membrane Based on a Molecular Simulation Technique and Permeation Model.* J. Phys. Chem. B., 2000. **104**: p. 1971.
42. Sanemasa, I.A., Y., *Association of Benzene and Alkylbenzenes with Cyclodextrins in Aqueous Medium.* Bull. Chem. Soc. Jpn., 1987. **60**: p. 2059.
43. Krishna, R., *A United Approach to the Modeling of Intraparticle Diffusion in Adsorption Processes.* Gas Sep. Purif., 1993. **7**: p. 91.